



**UNIVERSITÀ DEGLI STUDI DI PADOVA**  
**LEOPOLD-FRANZENS UNIVERSITÄT INNSBRUCK**  
**ALBERT-LUDWIGS UNIVERSITÄT FREIBURG**

*HOME INSTITUTION:* UNIVERSITÀ DEGLI STUDI DI PADOVA,  
DIPARTIMENTO DI FARMACOLOGIA ED ANESTESIOLOGIA

*HOST INSTITUTION:* LEOPOLD-FRANZENS UNIVERSITÄT INNSBRUCK,  
INSTITUT FÜR BIOCHEMISCHE PHARMAKOLOGIE

*HOST INSTITUTION:* ALBERT-LUDWIGS UNIVERSITÄT FREIBURG,  
INSTITUT FÜR EXPERIMENTELLE UND KLINISCHE PHARMAKOLOGIE  
UND TOXIKOLOGIE

*DOCTORAL DISSERTATION*  
*in*

**“MOLECULAR AND CELLULAR PHARMACOLOGY”**  
**“FARMACOLOGIA MOLECOLARE E CELLULARE”**  
**SSD: BIO/14**

DOCTORAL PROGRAMME  
XX CICLE

***Assessing the molecular basis for rat-selective induction of the  
mitochondrial permeability transition by norbormide***

COORDINATOR: *Prof. Sisto Luciani*

Department of Pharmacology and Anesthesiology, University of Padova

SUPERVISOR: *Prof. Sergio Bova*

Department of Pharmacology and Anesthesiology, University of Padova

EXTERNAL SUPERVISOR: *Dott. Fernanda Ricchelli*

C.N.R., Institute of Biomedical Technologies/Padova Unit, Department of  
Biology, University of Padova

DOCTORAL CANDIDATE : Alessandra Zulian

31 January, 2008



# INDEX

SUMMARY.....	1
RIASSUNTO.....	2
ABBREVIATIONS.....	3
1. MITOCHONDRIA.....	5
1.1. Structure of mitochondria.....	5
1.2. Bioenergetics of Mitochondria.....	6
1.3. Mitochondria and cell death.....	9
2. PERMEABILITY TRANSITION PORE (PTP).....	14
2.1. Regulation of the PTP.....	14
2.2 Molecular nature of the PTP.....	16
2.3. Formation of the PTP .....	20
2.4. The PTP in pathology.....	21
3. NORBORMIDE.....	23
3.1. Chemistry.....	23
3.2. Pharmacological effects.....	24
3.3. Mitochondrial effects.....	27
4. AIM OF THE STUDY.....	29
5. MATERIAL AND METHODS.....	31
5.1. Materials.....	31
5.2. Methods.....	31
5.2.1. Isolation of mitochondria and determination of mitochondrial proteins.....	31
5.2.2. Mitochondrial oxygen consumption (RCR test).....	32
5.2.3. Mitochondrial permeability transition (PT). Matrix swelling as measured by <i>light-scattering(LS)</i> changes.....	34

5.2.4. Mitochondrial permeability transition (PT). Release of matrix $\text{Ca}^{2+}$ as measured by the <i>calcium retention capacity</i> (CRC) with a $\text{Ca}^{2+}$ fluorescent probe, Calcium Green-5N.....	35
5.2.5. Mitochondrial permeability transition (PT). Collapse of the membrane potential as measured by the fluorescence changes of pyronin G, a probe of membrane potential.....	36
5.2.6. Fluorescence anisotropy measurements.....	38
6. RESULTS.....	45
6.1. Species-specific modulation of the mitochondrial PT by NRB.....	45
6.2. Correlation between vasoconstrictor activity (toxic effect) of NRB and regulation of mitochondrial PT.....	47
6.3. “The active core” of NRB molecule.....	50
6.4. Mechanisms of species-selectivity towards the PT: species-specific differences in PTP structure or rather in drug transport.....	53
6.4.1. “Target” of NRB in the PTP. Experiments with cationic derivatives of NRB.....	53
6.4.2. Transport modality of NRB into mitochondria. Fluorescence anisotropy measurements.....	58
7. DISCUSSION.....	63
8. BIBLIOGRAPHY.....	67





## SUMMARY

It was recently demonstrated that the rat-selective toxicant norbormide also induces rat-selective opening of the permeability transition pore (PTP) in isolated mitochondria. Norbormide is a mixture of *endo* and *exo* stereoisomers; however, only the *endo* forms are lethal to rats. In the present study we tested both *endo* and *exo* isomers as well as neutral and cationic derivatives of norbormide to: (i) verify if the PTP-regulatory activity by norbormide is stereospecific; (ii) define the structural features of norbormide responsible for PTP-activation, (iii) elucidate the basis for the drug species-specificity. Our results show that: (i) Norbormide isomers affect PTP in a rat-selective fashion; however, no relevant differences between lethal and non-lethal forms are observed suggesting that drug regulation of PTP-activity and lethality in rats are unrelated phenomena; (ii) A (phenylvinyl)pyridine moiety represents the key element conferring the PTP-activating effect; (iii) Cationic derivatives of rat-active compounds accumulate in the matrix *via* the membrane potential and activate the PTP also in mouse and guinea pig mitochondria. These findings suggest that the norbormide-sensitive PTP-target is present in all species examined, and is presumably located on the matrix side. The species-selectivity may depend on the unique properties of a transport system allowing drug internalisation in rat mitochondria.

## RIASSUNTO

E' stato recentemente dimostrato che la norbormide (NRB), un agente tossico selettivo per il ratto, è in grado di indurre anche l'apertura del poro di transizione di permeabilità (PTP) in maniera ratto-specifica in mitocondri isolati. La NRB è una miscela di *endo* ed *exo* stereoisomeri; tuttavia, solo le forme *endo* sono risultate essere letali per i ratti. Nel presente studio sono stati analizzati sia gli *endo* che gli *exo* isomeri così come derivati neutri e cationici della NRB allo scopo di: (i) verificare se l'attività regolatoria della NRB sul PTP è stereospecifica; (ii) definire le caratteristiche strutturali della molecola della NRB responsabili della attivazione del PTP; (iii) spiegare le basi della attività specie-specifica della NRB. I nostri risultati dimostrano che: (i) gli isomeri della NRB attivano il PTP con un effetto selettivo per il ratto; comunque, non sono state riscontrate differenze rilevanti tra gli isomeri letali e non letali suggerendo che la regolazione del PTP indotta dalla NRB e l'effetto letale nei ratti sono due fenomeni non correlati; (ii) il gruppo (fenilvinil)piridina rappresenta l'elemento chiave della molecola di NRB responsabile dell'effetto attivatorio del PTP; (iii) i derivati cationici dei composti attivi sul ratto si accumulano all'interno della matrice del mitocondrio grazie al potenziale di membrana e sono in grado di attivare il PTP anche nei mitocondri di topo e di cavia. Questi risultati suggeriscono che il target nel PTP sensibile all'effetto della NRB è presente in tutte le specie animali esaminate, e questo target è probabilmente localizzato nel lato di matrice della membrana mitocondriale. La specie-selettività potrebbe dipendere dall'esistenza di un sistema di trasporto che permetterebbe l'internalizzazione della NRB solo nei mitocondri di ratto.



## ABBREVIATIONS

<b>ADP</b>	adenosindiphosphate
<b>ANT</b>	adenine nucleotide translocase
<b>ATP</b>	adenosintriphosphate
<b>CRC</b>	calcium retention capacity
<b>CsA</b>	cyclosporin A
<b>Cyt-C</b>	cytrocrome <i>c</i>
<b>CyP-D</b>	cyclophilin D
<b>DNA</b>	deoxyribonucleic acid
<b>DPH</b>	1,6-diphenyl-1,3,5-hexatriene
$\Delta\mu_{\text{H}}$	electrochemical proton gradient
$\Delta\text{pH}$	chemical gradient
$\Delta\Psi_{\text{m}}$	membrane potential
<b>FADH<sub>2</sub></b>	1,5-dihydro- flavin adenine dinucleotide
<b>HK</b>	hexokinase
<b>IMM</b>	inner mitochondrial membrane
<b>MtCK</b>	mitochondrial creatine kinase
<b>NADH</b>	nicotinamide adenine dinucleotide
<b>NRB</b>	norbormide
<b>OMM</b>	outer mitochondrial membrane
<b>OXPHOS</b>	oxidative phosphorylation
<b>PN</b>	pyridine nucleotides
<b>PBR</b>	peripheral benzodiazepine-type receptor
<b>PT</b>	permeability transition
<b>PTP</b>	permeability transition pore
<b>RNA</b>	ribonucleic acid
<b>ROS</b>	reactive oxygen species
<b>TMA-DPH</b>	1-(4-trimethylammoniumphenyl)-6-phenyl-1,3,5-hexatriene



## 1. MITOCHONDRIA



**Figure 1. Electron micrograph of a mitochondrion.** The inner membrane, which surrounds the matrix space, shows many invaginations, called cristae. Small calcium-containing matrix granules also are evident.

### 1.1. Structure of mitochondria

Mitochondria have crucial roles in diverse cellular functions, such as energy production, modulation of redox status, osmotic regulation,  $\text{Ca}^{2+}$  homeostasis, inter-organelle communication, cell proliferation and senescence, and cell responses to a multiplicity of physiological and genetic stresses. They also orchestrate a wide number of signals to determine cell commitment to death or survival.

Mitochondria are tubular organelles that often form a deeply interconnected network in the cell (Skulachev, 2001). They are among the largest organelles in the cell, each one being about the size of an *E. coli* bacterium. Most eukaryotic cells contain many mitochondria, which collectively can occupy a 25 percent of the volume of the cytoplasm. They are large enough to be seen under a light microscope, but the details of their structure can be viewed only by electron microscopy (Fig.1) and by the electron microscopic tomography (Mannella, 2000).

Mitochondria contain two membrane systems that differ in composition and function: the *outer* (OMM) and the *inner* (IMM) mitochondrial membrane.

The OMM, composed of about half lipids and half proteins, defines the smooth outer perimeter of the mitochondrion. It contains integral proteins called *porins* that render the membrane permeable to molecules of about 5000 dalton or less. Larger molecules can traverse the OMM only by active transport through

*mitochondrial membrane transport proteins* (Crompton, 1999; Nicholls, 2005).

The outer membrane also contains enzymes involved in such diverse activities as the elongation of fatty acids, the oxidation of ephinephrine (adrenaline) and the degradation of tryptophan.

In contrast, the IMM is a membrane impermeable to most solutes, with a much larger extension than that of the OMM. The IMM is freely permeable only to oxygen and carbon dioxide. It contains many enzymes including those of the electron transport system and of the ATP synthetase complex. Its structure is highly complex showing numerous invaginations called *cristae*. The cristae form sheets and tubes by invagination of the inner membrane and connect to the outer membrane through relatively small uniform tubular structures that Perkins and co-workers called *cristae junctions*, with a diameter of approximately 28 nm (Perkins and Frey, 2000). The formation of tubular cristae and crista junctions is a dynamic process, which might be sensitive to or controlled by the matrix volume and by the energetics of protein-lipid membrane folding (Frey *et al.*, 2000). There is considerable evidence that the IMM is a dynamic structure able to change shape rapidly in response to alterations in osmotic or metabolic conditions. The structural changes might be more than a passive volume adjustment; they could be an integral part of feed-back mechanisms by which mitochondria respond to environmental perturbations (Frey & Mannella, 2000).

The IMM and OMM define two submitochondrial compartments: the *intermembrane space* between the outer and the inner membrane with its cristae, and the *matrix*, or central compartment (Fig 2). The matrix includes enzymes of intermediary metabolism and multiple copies of a genome that encodes for a few inner membrane proteins, and the RNAs<sub>s</sub> needed for their translations. The several hundred other proteins in the mitochondrion are encoded by nuclear DNA and are synthesized in and imported from the cytosol.

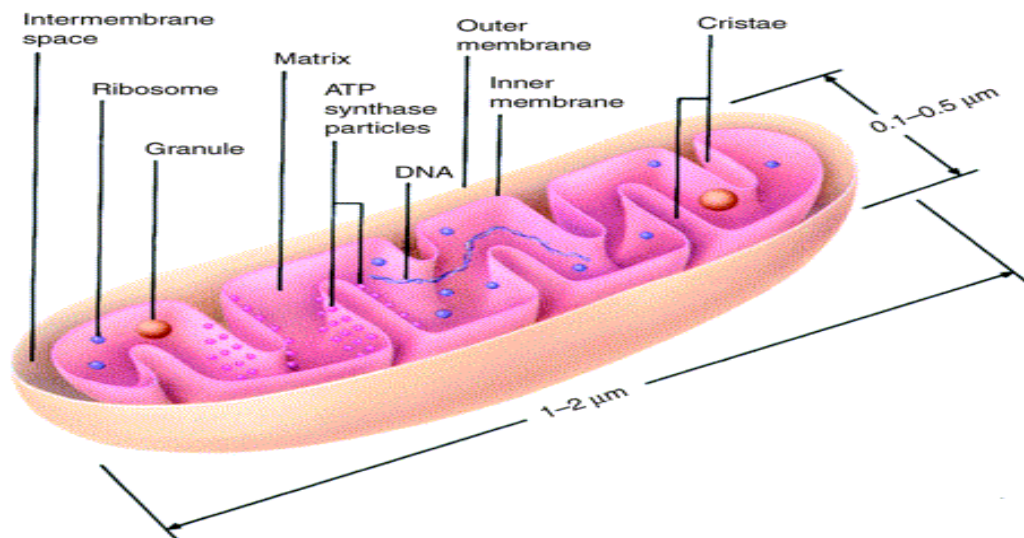


**Figure 2.** *A model of mitochondrion (from: Frey & Mannella, 2000).*

## 1.2. Bioenergetics of Mitochondria

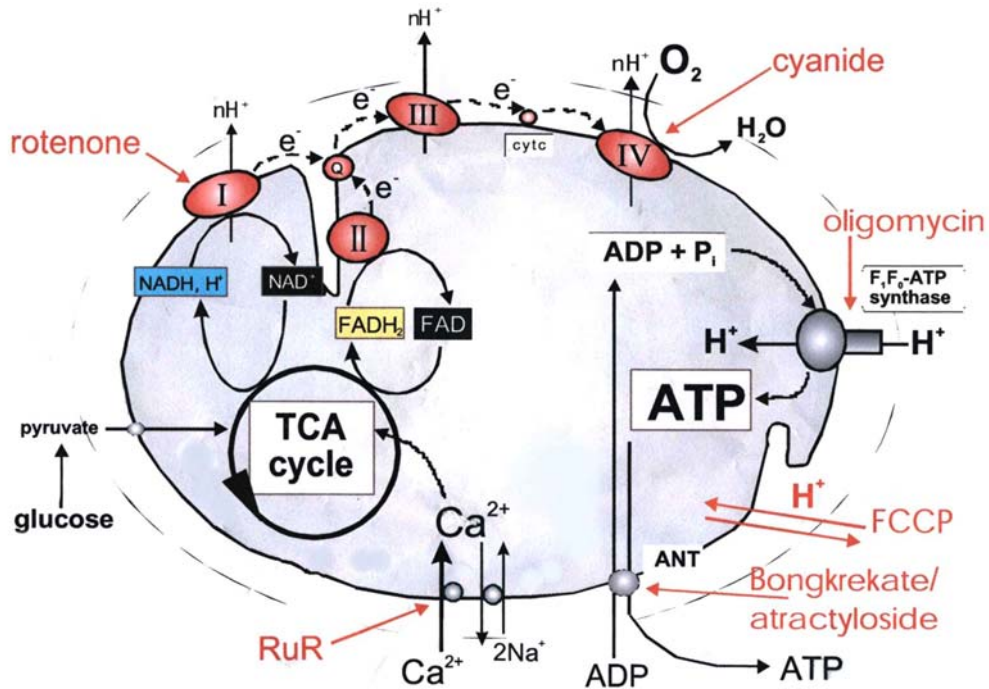
Mitochondria generate ATP, the major currency used by cells in energy-requiring processes, through the primary function of mitochondria, which is the *oxidative phosphorylation* (OXPHOS). The IMM is the site of this process, including in its structure all the complexes of the electron transport system and the ATP synthase complex. In accordance with the chemiosmotic theory mitochondria convert the electron flux through membrane complexes of the inner membrane into a proton gradient to run the endoergonic reaction of ATP synthesis.

Fig 3. shows a cartoon of a mitochondrion which illustrates the chemiosmotic principle that governs the process of oxidative phosphorylation. The supply of substrate, such as the product of glycolysis, pyruvate, to the citric acid cycle maintains the reduced state of the pyridine nucleotide (NADH) and the flavoprotein, (FADH<sub>2</sub>) pools. These reducing equivalents are supplied to the respiratory chain, NADH to complex I and FADH<sub>2</sub> from succinate-linked substrates to complex II. Electrons are transported from either Complex I or Complex II via ubiquinone to Complex III and are ultimately transferred to oxygen at cytochrome c oxidase (Complex IV), generating H<sub>2</sub>O. During the

coupled redox reactions of Complexes I-IV, protons are translocated across the IMM to the intermembrane space, generating an electrochemical proton gradient ( $\Delta\mu_H$ ). Rigorously, the proton motive force, which provides proton influx, is composed of a chemical ( $\Delta p_H$ ) and an electrical ( $\Delta\Psi_m$ ) component, according to the Nerst equation:

$$\Delta\mu_H = zF \Delta\Psi_m + RT \ln [H^+]_{in} / [H^+]_{out}$$

$\Delta p_H$  in mammalian cells is about 0.5-1, which correspond to 30-60mV;  $\Delta\Psi_m$ , in the order of 180-200 mV (inside-negative), is the major component of the proton motive force (Nichols and Ferguson, 1992).  $\Delta\Psi_m$  provides the driving force for proton influx through the  $F_1F_0$ -ATP synthase. The  $F_0$  component of this enzyme system acts essentially as a proton conductance channel in which the protons, following the electrochemical potential gradient, activate the  $F_1$  complex, allowing the phosphorylation of ADP. Ultimately, ATP is generated and transported to the cytosol (Noji *et al.*, 1997). ATP produced in the matrix is exchanged with cytoplasmic ADP by the *adenine nucleotide translocase* (ANT).



**Figure 3. Cartoon illustrating the chemiosmotic principles that govern mitochondrial oxidative phosphorylation.**

The mitochondrial potential also provides the driving force for  $\text{Ca}^{2+}$  uptake into mitochondria through the  $\text{Ca}^{2+}$  uniporter. Indeed, an obvious corollary of the chemiosmotic theory is that  $\text{Ca}^{2+}$  fluxes across the ion-impermeable inner membrane are greatly favoured: based on the Nerst equation (and considering a  $\Delta\Psi_m$  of  $-180$  mV), the equilibrium would be reached only when  $\text{Ca}^{2+}$  in the matrix reaches a value  $10^6$  higher than that in the extramitochondrial space, i.e. in the cytosol. Thus, in studies carried out with isolated organelles, the rapid uptake of  $\text{Ca}^{2+}$  into the energized mitochondria could be directly demonstrated (Bernardi, 1999).

Inhibition of the respiratory chain or collapse of the electrochemical gradient abolishes the capacity of mitochondria to accumulate  $\text{Ca}^{2+}$ . For example, collapse of the  $\Delta\mu_H$  by protonophores, such as p-[trifluoromethoxyl]-phenyl- hydrazine (FCCP), inhibits the mitochondrial  $\text{Ca}^{2+}$  uptake both in vivo and in isolated organelles. The pharmacological and/or biochemical manipulation of these pathways is central to investigation of mitochondrial function. Based on these studies, it was assumed that in the signalling processes involving  $\text{Ca}^{2+}$  mitochondria would play a very active role.

### **1.3. Mitochondria and cell death**

The cell death is an essential physiological process that it is required for the normal development and maintenance of tissue homeostasis. When misregulated, it can contribute to various diseases including cancer and autoimmune and neurodegenerative diseases.

Two different mechanisms of cell death have been described: necrosis and apoptosis. The morphologic characteristics of the cells during the two death processes are different. During necrosis the cell swells, its mitochondria dilate, other organelles dissolve and the plasma membrane rupture causes release of cytoplasmic material. This often elicits an inflammatory response. By contrast, during apoptosis the cytoplasm shrinks and the chromatin condenses, but the organelles retain their integrity. The plasma membrane blebs and exposes phosphatidylserine, normally retained in the inner leaflet, on its outer surface. However, the plasma membrane does not rupture, preventing the release of

cellular compounds into the extracellular medium. Apoptotic cells ultimately fragment into membrane-enclosed vesicles (apoptotic bodies); *in vivo*, they are recognized and removed by phagocytes, thereby avoiding inappropriate inflammation. Biochemical hallmarks of apoptosis also include the activation of endonucleases, DNA degradation into oligonucleosomal fragments and the activation of cysteine proteases called caspases (Desagher and Martinou, 2000).

It is universally recognized that mitochondria play a key role in the events leading to both necrotic and apoptotic cell death.

Mitochondrial dysfunction can cause ATP depletion and excessive production of reactive oxygen species (ROS), which can lead to protein and lipid oxidation. Loss of ATP and oxidative damages in the injured tissues are typical events of cell necrosis (Orrenius, 2007).

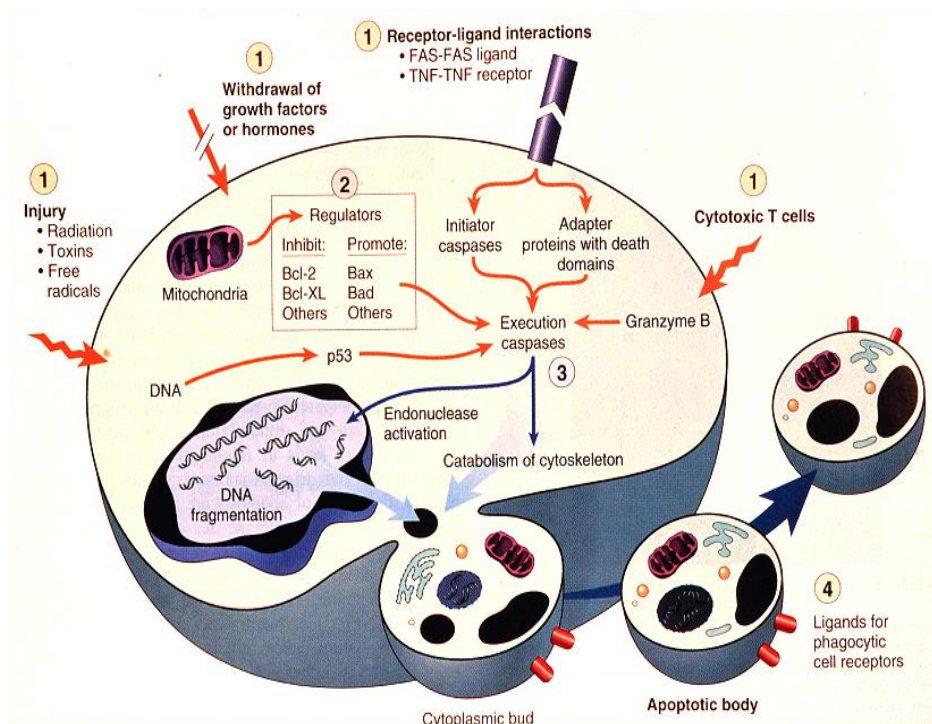


**Figure 4. Cell stimuli and events leading to apoptosis** (College of Veterinary Medicine-University of Florida: Illustrated Lecture Notes)

Mitochondria contain several cytotoxic proteins which can trigger apoptosis. During apoptosis, various proteins that are normally sequestered in the intermembrane space are released into the cytosol : cytochrome *c* (cyt *c*, a caspase activator), apoptosis-inducing factor (AIF; a nuclease activator), endonuclease G, high temperature requirement A2 (HtrA2/Omi), and second mitochondria



derived activator of caspase/direct IAP binding protein with low pI (Smac/DIABLO, a caspase co-activator).

Mitochondria can also interact with extramitochondrial proteins involved in the apoptotic process, such as the members of the Bcl-2 family (Fig. 4). In particular, the Bcl-2-related proteins display either anti-apoptotic and pro-apoptotic function. The anti-apoptotic members (e.g., Bcl-2 and Bcl-X<sub>L</sub>), which are localized in the OMM, promote the cell survival. Actually, they are present in large amount in tumour cells. Many pro-apoptotic members, such as Bax and Bad (in the cytosol) and others, present in the microtubules, mediate their effects *via* interaction with Bcl-2 and Bcl-X<sub>L</sub> or directly with the OMM. The main mechanism by which Bcl-2 family proteins regulate apoptosis is probably by modulating the cyt-*c* release. Cyt-*c* released into the cytosol binds to Apaf-1 (apoptotic protease-activating factor 1) and, in the presence of ATP or dATP, activates the pro-caspase 9, then forming all together a complex named apoptosome. This complex recruits and activates caspase 9, which, in turn, can activate other caspases (caspase cascade) (Fig 5).

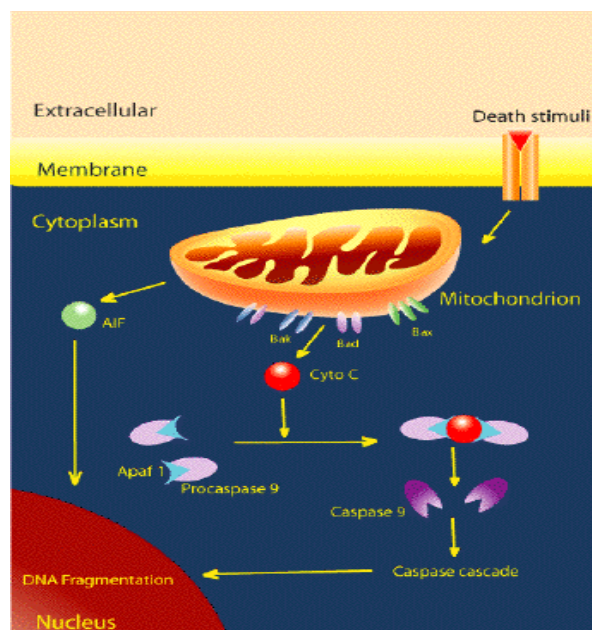


**Figure 5.**  
**Mitochondria and apoptosis**  
([www.mitosciences.com](http://www.mitosciences.com))

The mechanisms by which cyt-*c* and other apoptogenic proteins are released from the intermembrane space are not completely understood. Since the size of these factors largely exceeds the OMM pore diameter, some alternative form of OMM permeabilization is mandatory for their release. Although several models were proposed to explain the process, two mechanisms prevailed, namely, the direct

OMM permeabilization model and the permeability transition (PT) model. In the former, proapoptotic Bcl-2 family proteins such as Bax and Bad promote, directly or indirectly (by Bax/Bad-lipids or Bax/Bad-VDAC channels), the opening of pores on the OMM that are large enough to allow the channelling of apoptogenic proteins (Fig. 6). In the latter, rupture of the OMM and release of the intermembrane space components follow the opening of an inner membrane protein channel termed the permeability transition (PT) pore (PTP) (Fig. 6).

According to the direct OMM permeabilization model, channels would be formed after insertion into OMM of soluble Bax and/or Bax-related proapoptotic proteins (Saito et al, 2000). Consistent with this model, it was shown that several members of Bcl-2 family exhibit structural analogies with protein domains of diphtheria toxin and bacterial colicins, which can form functional ionic channels in synthetic model membranes (Shendel et al., 1998). However, in most cases, channel activities were recorded in non-physiological conditions and their relevance, if any, in apoptosis signaling remains undetermined.

As about the alternative model, the mitochondrial PT can be defined as a sudden increase of IMM permeability to solutes with molecular mass up to 1500 Da, and is due to the opening of a voltage- and  $\text{Ca}^{2+}$ -dependent, cyclosporin A (CsA)-sensitive, high-conductance protein channel, the **PT pore** (PTP) (Zoratti and Szabo, 1995; Bernardi, *et al.* 2001) (see next paragraphs). In its fully open state the apparent diameter of the PTP is about 3 nm.

The primary consequence of a prolonged PTP opening is mitochondrial depolarization due to equilibration of the proton gradient, which may be followed by respiratory inhibition, as matrix pyridine nucleotides (PN) are lost. Equilibration across the IMM of ions and solutes with molecular mass below the pore size induces massive release of the  $\text{Ca}^{2+}$  stored in the matrix and extensive swelling of mitochondria, given the colloidal osmotic pressure exerted by the high concentration of matrix proteins. As a consequence, the unrestricted cristae unfolding causes breaches in the OMM and release of intermembrane proteins. However, it is important to underline that PTP openings can induce rupture of the OMM only as a result of matrix swelling and therefore cyt-*c* and the other apoptogenic molecules do not exit mitochondria through the PTP itself (Bernardi *et al.* 2007). Among various effectors (see next paragraphs), members of Bcl-2

family can regulate opening of the PTP by binding to some of the pore constituents ( Kroemer, 1997).

The PT-based model for OMM permeabilization is supported by a number of observations: i) studies with experimental models have evidenced a  $\Delta\Psi_m$  collapse before caspase activation (Kroemer *et al.*, 1998); ii) the specific inhibitor of the PTP, CsA, as well as other inhibitors, exerts a protective effect towards several apoptotic responses (Kroemer *et al.*, 1998; Zamzami and Kroemer, 2001); iii) several bacterial and viral proteins that modulate apoptosis interact with PTP components (Zamzami and Kroemer, 2001).

However, conflicting data question whether PTP opening is the cause or the consequence of cyt-*c* leakage from mitochondria. Actually, some studies would indicate that cyt-*c* release can occur in the absence of or before  $\Delta\Psi_m$  disruption (Bossy- Wetzel *et al.*, 1998). Moreover, the hypothetical PT-based mechanism conflicts with another model of matrix swelling implicating an initial hyperpolarization of the inner membrane that precedes cyt-*c* release in some systems (Fig. 6). According to Vander Heiden *et al.* (1999), this hyperpolarization might result from the inability to exchange mitochondrial ATP with cytosolic ADP during apoptosis. This antiport is normally mediated by VDAC and ANT. Impairment of ATP-ADP exchange by VDAC closure should inhibit  $F_0F_1$ -ATPase activity, resulting in an inhibition of  $H^+$  re-entry to the matrix, and should thereby contribute to the hyperpolarization of the IMM. Such an increase of the mitochondrial transmembrane potential is predicted to promote an osmotic matrix swelling.

It is very important to understand that the different models of OMM permeabilization are not necessarily mutually exclusive, and the possibility exists that different mechanisms may cause the release of intermembrane space proteins in different apoptotic conditions and cell types (Rasola and Bernardi, 2007).

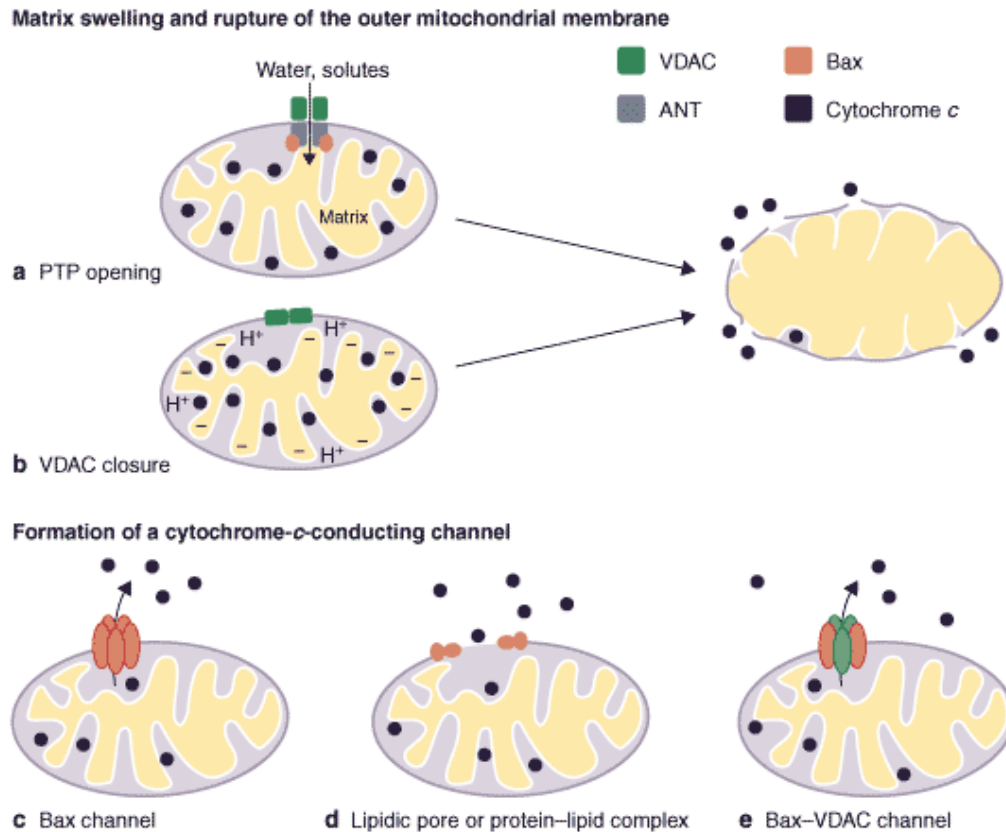


**Figure 6. Models for the release of cytochrome *c* (and other apoptogenic factors) from mitochondria.**

During the process of apoptosis, cytochrome *c* is released from mitochondria into the cytosol. In models *a* and *b*, the outer mitochondrial membrane ruptures as a result of matrix swelling, allowing cytochrome *c* to escape from mitochondria. Model *a* involves opening of the permeability transition pore (PTP) whereas model *b* involves closure of the voltage-dependent anion channel (VDAC) and hyperpolarization of the IMM as the causes of mitochondrial-matrix swelling. In models *c-e*, a large channel forms in the OMM, allowing cytochrome *c* release, but mitochondria are not damaged. (ANT, adenine-nucleotide translocator).

## 2. PERMEABILITY TRANSITION PORE (PTP)

### 2.1. Regulation of the PTP

The pore open–closed transitions are highly regulated by multiple effectors that may converge on a smaller set of regulatory sites. Below, the factors that affect the PT are classified into matrix and membrane effectors (for a review, see Bernardi *et al.*, 2006; Rasola *et al.*, 2007).

### **Matrix effectors**

Pore opening is favored by **matrix  $\text{Ca}^{2+}$**  through a site that can be competitively inhibited by other  $\text{Me}^{2+}$  ions, such as  $\text{Mg}^{2+}$ ,  $\text{Sr}^{2+}$  and  $\text{Mn}^{2+}$ , and by  $\text{P}_i$  through a still-undefined mechanism. External divalent metal ions, including  $\text{Ca}^{2+}$ , all decrease the probability of pore opening (Zamzami *et al.*, 2001 ). Pore opening is strongly promoted by an **oxidized state of pyridine nucleotides** (PN, NADH/ $\text{NAD}^+$  and NADPH/ $\text{NADP}^+$ ) (Costantini *et al.*, 1996), and **of critical dithiols** (vicinal thiols in cysteinyl (Cys) residues) at discrete sites, and both effects can be individually reversed by proper reductants. Dithiol-disulfide interconversion (as well as dithiol cross-linkage) at a critical site (dubbed the “S-site”) is associated with a higher probability of PT activation through a change of the threshold potential at which pore opening occurs (Petronilli *et al.*, 1994; Costantini *et al.*, 1996). Numerous literature data identify the ANT domains exposed to the matrix side as the pore constituents containing the relevant vicinal thiols (**internal thiols**) (Costantini *et al.*, 2000; Halestrap *et al.*, 1997; Halestrap *et al.*, 2002; Kanno *et al.*, 2004; Kowaltowski *et al.*, 1997; McStay *et al.*, 2002). In addition, a class of pore-regulating thiols, which are sensitive to membrane-impermeant reagents and are not located on the ANT, has been also evidenced (**external thiols**) (Kowaltowski *et al.*, 1997; Costantini *et al.*, 1998). The protein(s) which binds external thiols has not yet been identified.

The PT is strictly modulated **by matrix pH**. In de-energized mitochondria, the pH optimum for opening is 7.4, while the open probability decreases sharply both below pH 7.4 (through reversible protonation of critical histidyl residues that can be blocked by diethylpyrocarbonate, DEPC) and above pH 7.4 (through an unknown mechanism) (Nicolli *et al.*, 1993).

Opening of the PTP is inhibited by the immunosuppressant **cyclosporin A (CsA)** after binding to CyP-D, a matrix peptidyl-prolyl *cis-trans* isomerase. The relevant binding sites of CyP-D for CsA display a very high affinity, the estimated  $K_d$  being between 5 and 8 nM (Halestrap and Davidson, 1990). The immunosuppressive effects of CsA are caused by a  $\text{Ca}^{2+}$ -calmodulin-dependent inhibition of calcineurin (a cytosolic phosphatase), due to the complex of the drug with cytosolic CyP-A. In turn, this prevents dephosphorylation and nuclear

translocation of nuclear factors of activated T cells and other transcription factors that are essential for the activation of T cells. Available evidence suggests that calcineurin is not involved in the effects of CsA on the PTP because CsA derivatives have been described that bind CyP-D and desensitize the pore, but do not inhibit calcineurin.

### ***Membrane effectors***

The inside-negative  $\Delta\psi_m$  tends to stabilize the PTP in the closed conformation. It has been postulated the existence of a voltage sensor that decodes the changes of both the **transmembrane voltage** and of the **surface potential** into changes of the PTP open probability (Petronilli *et al.*, 1993). Such a sensor would easily account for pore opening following depolarization as such, and for the effects of a large variety of membrane-perturbing agents that can either inhibit or promote the PT. In general, amphipathic anions, such as fatty acids produced by phospholipase A<sub>2</sub>, favor the PT with an effect that cannot be explained by depolarization. In particular, arachidonic acid appears to play a key role in apoptotic Ca<sup>2+</sup>-dependent apoptotic signalling through the PTP. Conversely, polycations such as spermine, amphipathic cations such as sphingosine and trifluoroperazine, and positively charged peptides, inhibit pore opening. The putative voltage sensor may comprise critical arginine residues, as suggested by modulation of the PTP voltage dependence by a set of arginine-selective reagents (Johans *et al.*, 2005).

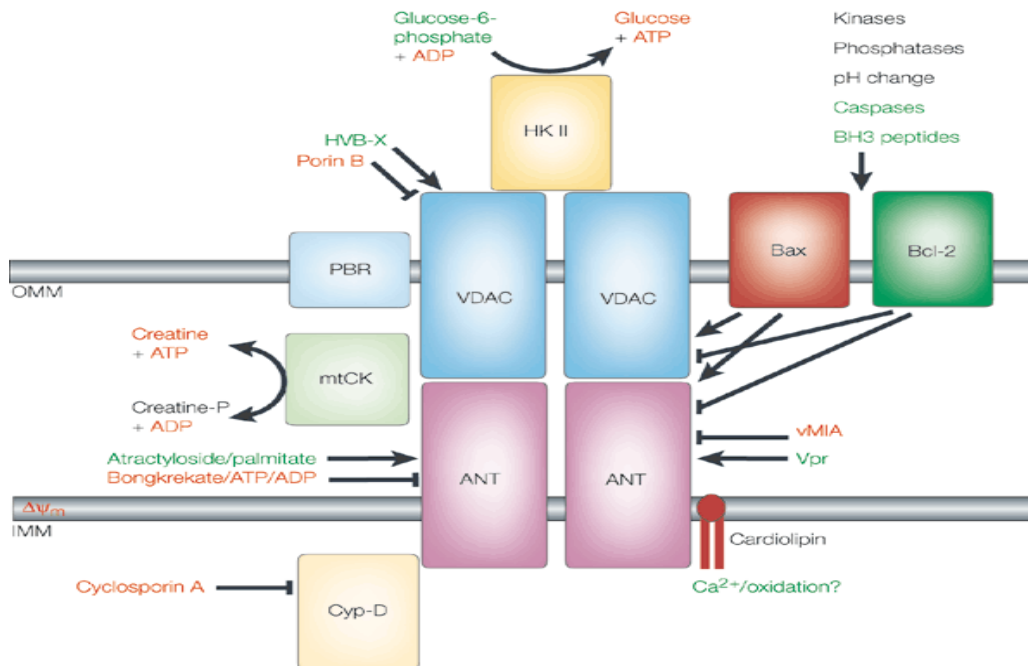
The PTP is regulated by **electron flux within respiratory chain complex I**, with an increased opening probability when flux increases (Fontaine *et al.*, 1998 ).

## **2.2 Molecular nature of the PTP**

A passionate debate surrounds the molecular composition of the PTP, which at presently remains unclear. Recent genetic data have challenged popular views on the molecular nature of the PTP, and called into question many early conclusion about its structure.

A restricted set of proteins was proposed to take part in the PTP. These include: the IMM adenine nucleotide translocator (**ANT**); the large and unselective OMM

voltage-dependent anion channel (**VDAC**); the OMM peripheral benzodiazepine-type receptor (**PBR**), and the matrix cyclophilin D (**CyP-D**), a mitochondrial member of the cyclophilin family that is the target of the desensitising effects of CsA on the PTP (Fig. 7).



Nature Reviews | Molecular Cell Biology

**Figure 7. Hypothetical molecular architecture of the permeability transition pore complex and its regulation.** (Zamzami & Kroemer, 2001). The PTP complex involves several transmembrane proteins: the ANT, the VDAC and the PBR. It also involves members of the Bax/Bcl-2 family, as well as associated proteins such as HK II, mtCK and the peptidyl-prolyl isomerase Cyp-D. The VDAC functions as non-specific pore, allowing diffusion of solutes up to 5 kDa. The ANT is responsible for exchange of ATP and ADP on the IMM. Agents or metabolites labelled in green facilitate PTP opening; agents in red inhibit pore opening. Proteins or peptides carrying the Bcl-2 homology region-3 (BH3) motif may act on either Bax or Bcl-2 (or their homologues) in the OMM.  $\text{Ca}^{2+}$  has been postulated to act on ANT-associated cardiolipin molecules; CsA acts on Cyp-D. HIV-1 Vpr, the viral mitochondrial inhibitor of apoptosis (vMIA), hepatitis virus B X-protein (HVB-X), and *Neisseria meningitidis* porin B also act on the PTP. (OMM, outer mitochondrial membrane; IMM, inner mitochondrial membrane;  $\Delta\psi_m$ , electrochemical proton gradient).

Additional proteins that may play a regulatory role, but are generally not considered as part of the pore itself, are both antiapoptotic and proapoptotic **Bcl-2 family** members on the OMM; mitochondrial creatine kinase (**MtCK**), which shuttles high-energy phosphate groups in the intermembrane space of muscle and

heart mitochondria, and mitochondrial hexokinase (**HK**), which catalyses the first step of glycolysis.

### ***Adenine nucleotide translocator***

The PTP is modulated by ligands of the ANT. Atractylate, which inhibits the ANT and stabilizes it in the “c” (cytosol-facing) conformation, favors PTP opening, while bongkrekate, which also inhibits the ANT but stabilizes it in the “m” (matrix-facing) conformation, favors PTP closure ( Shultheiss et al., 1984).

These findings led to the suggestion that the PTP may be directly formed by the ANT. Indeed, unequivocal evidence that the ANT is not essential for PTP formation was obtained in a detailed analysis of liver mitochondria prepared from mice lacking all ANT isoforms. The ANT <sup>-/-</sup> mitochondria underwent a Ca<sup>2+</sup>- and oxidant-dependent, CsA-sensitive PT with matrix swelling, indicating that the ANT is neither the obligatory binding partner of CyP-D nor the site of action of oxidants (Kokoszka et al., 2004).

### ***Voltage-dependent anion channel***

The earliest indication that the OMM could be involved in the PT was the finding that swelling induced by sulfhydryl reagents is not observed in mitoplasts, *i.e.*, mitochondrial preparations lacking the OMM. Several lines of evidence suggest that the outer membrane component of the PTP is VDAC. Indeed, purified VDAC forms channels with a pore diameter of 2.5-3.0 nm that possess electrophysiological properties similar to those of the PTP ( Szabo, 1993); VDAC is modulated by many factors that also affect the PTP, such as NADH, Ca<sup>2+</sup>, glutamate and hexokinase (Gincel *et al*, 2004). It should be noted that these analogies do not represent a proof of mechanism, and that the PTP of mitochondria prepared from VDAC <sup>-/-</sup> mice was indistinguishable from the PTP of strain-matched, wild-type mitochondria ( Krauskopf, 2006).

### ***Cyclophilin D***

The most conclusive results on the role of CyP-D in regulation of the PTP were obtained after inactivation of the Ppif gene, that encodes CyP-D in the mouse (Basso *et al*, 2005; Nakagawa *et al*, 2005). In all these studies the Ca<sup>2+</sup> dependent PT still took place; CyP-D ablation increased the Ca<sup>2+</sup> load required to open the pore (which became identical to that of CsA-treated, strain-matched wild type



mitochondria); CsA had no effects on the PTP, which instead retained its normal response to other inhibitors. Taken together, these findings demonstrate that CyP-D is a regulator, rather than a component, of the PTP, whose structure is unlikely altered by the absence of CyP-D.

### ***Peripheral benzodiazepine receptor***

The PBR is an 18 kDa, highly hydrophobic protein located in the OMM. It was initially identified as the protein binding benzodiazepines in tissues that lack 4-aminobutyrate receptors, the clinical target of benzodiazepines in the central nervous system (CNS). The PBR shares no amino acid homology with CNS 4-aminobutyrate receptors, and can be distinguished pharmacologically from CNS receptors by its binding to a variety of high-affinity (~nM), specific ligands (Hirsch *et al.* 1998), notably the benzodiazepine, Ro5-4864, and the isoquinoline carboxamide, PK11195. The PBR is found in a variety of tissues at varying levels and is especially abundant in cells producing steroid hormones, such as adrenal cortex and Leyding cells of the testis. In these cells, PBR promotes the transport of cholesterol into the mitochondrial matrix. The PBR also binds some porphyrins, including protoporphyrin IX, a potent inducer of the PTP, with high affinity (Pastorino *et al.* 1994), and is thought to be involved in the transport of porphyrins into the mitochondrion.

Involvement of the PBR in PTP function was initially suggested following biochemical isolation of the PBR, which indicated a close association of this protein with VDAC and ANT. Moreover, high concentrations of PK11195 and Ro5-4864 stimulated the opening of the pore (Hirsch *et al.*, 1998; Chelli *et al.*, 2001; Li *et al.*, 2007). However, a conclusive evidence that PBR is involved in PTP structure has not yet been reached. The examination of mitochondria prepared from animals in which the expression of PBR had been eliminated by ‘knockout’ strategies would greatly help to clarify these issues. Unfortunately, initial attempts to generate such animals has indicated that nonconditional elimination of PBR expression results in embryonic lethality (Papadopoulos *et al.*, 1997). Thus, although it cannot be ruled out that the PBR is part of the PTP, conclusions based on the exclusive use of PBR ligands should, at this point, be viewed and interpreted with some caution until genetic tools are generated that will allow these questions to be addressed directly.

## 2.3. Formation of the PTP

He & Lemaster have proposed a model of PTP formation and gating in which the pore forms by aggregation of misfolded integral membrane proteins damaged by oxidants and other stresses, according with earlier models suggesting that the PT is not a consequence of the opening of a preformed pore, but rather the result of oxidative damage to membrane proteins (He and Lemaster, 2002). While interesting, this model fails to account for PTP regulation by voltage and by matrix pH, which is not easy to reconcile with a permeability pathway created by a heterogeneous set of denatured proteins. The popular idea is that the pore (a) forms at “contact site” between the IMM and OMM and (b) that it spans both membranes (Zamzami and Kroemer, 2001). It is important to understand that the idea that the PTP forms at contact sites (ANT/VDAC) is based on a set of assumptions rather than on established facts, and should be considered with great caution also because the very existence of points of fusion between the OMM and IMM has been questioned by tomography of unfixed mitochondria (Jennings and Ganote, 1976). The second point does not take into account that the permeability pathway resulting from a pore spanning both membranes would directly connect the matrix with the cytosol, resulting in the release of matrix solutes, but not of cytochrome *c* and of other intermembrane pro-apoptotic proteins. Bernardi *et al.* have proposed another model of interaction (Bernardi *et al.*, 2006). PT is primarily an inner membrane event that may cause secondary outer membrane changes, and that in an *in vivo* setting, the outer membrane can affect the probability of pore opening through protein-protein interactions, as exemplified in the scheme of Fig. 8. Interaction of an outer membrane protein (e.g. VDAC or the PRB) with the PTP might depend on a specific conformation, which could be conferred by cytosolic regulator(s) after modification by upstream signaling pathway(s). Binding would be followed by a conformational change that allows interaction with the PTP and its stabilization in the closed conformation (panel 1: note that the ligand-dependent change could instead favor the open conformation of the PTP and that intermembrane factors could also play a role, possibilities that are omitted for clarity). In the absence of outer membrane interactions, the PTP could flicker between the closed state (panel 2) and the open state (panel 3) under the

effect of inner membrane and matrix modulators such as the  $\Delta\Psi_m$ , pH, CyP-D,  $\text{Ca}^{2+}$  and PN. Stabilization of the open conformation could lead to the rearrangement of cristae structure and, eventually, to outer membrane rupture (panel 4). This scheme is meant as an example of how the OMM could confer regulatory features to the PTP without necessarily providing a permeability pathway for solute diffusion. As a matter of fact, with the exception of CsA, it is currently impossible to assign any pore effectors to a particular site, a key issue that will have to await PTP identification.

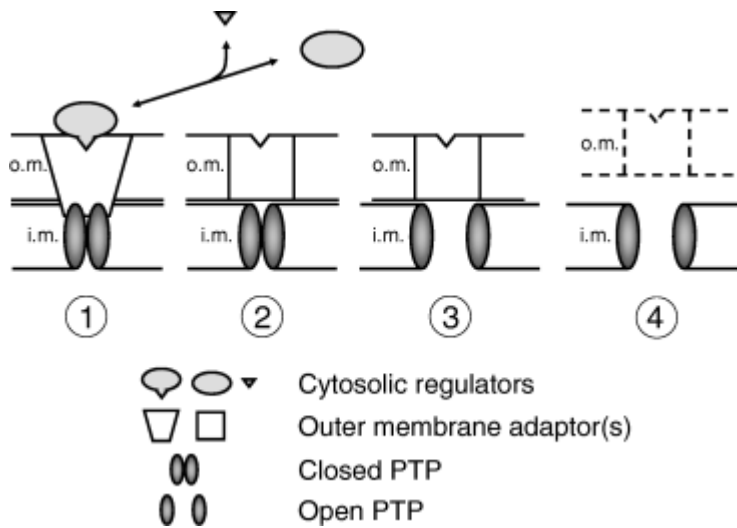


**Figure 8. Model for permeability transition pore (PTP) regulation by outer membrane proteins.** Hypothetical model of inner membrane (i.m.) PTP modulation by interaction with outer membrane (o.m.) proteins, which could be the target of cytosolic effector molecules. Broken lines denote outer membrane rupture following PTP openings of long duration. For explanation see the text.

## 2.4. The PTP in pathology

Mitochondria are involved in more than 40 known human diseases. The effect of CsA in treatment have implicated PTP-dependent mitochondrial dysfunction and  $\text{Ca}^{2+}$  deregulation in many of these conditions, including ischemia-reperfusion (I/R) injury of the heart, ischemic and traumatic brain damage, muscular dystrophy caused by collagen VI deficiency, amyotrophic lateral sclerosis,

acetaminophen hepatotoxicity, hepatocarcinogenesis by 2-acetylaminofluorene, and fulminant, death receptor-induced hepatitis.

Despite the uncertainties about its molecular composition, sound evidence indicates that the PTP plays a role in several diseases in vivo, and that the pore represents a viable target for drug development. Many well-characterized death signalling pathways affect mitochondrial function in a variety of ways, and these include modulation of the PTP.

### 3. NORBORMIDE

#### 3.1. Chemistry

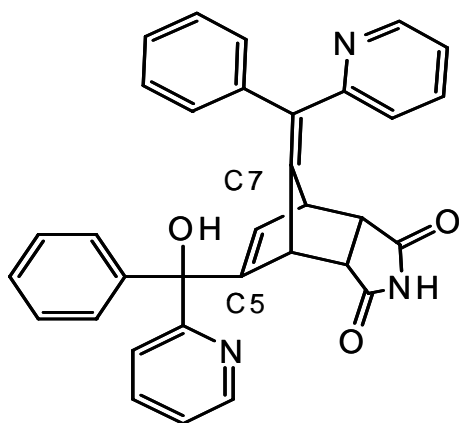


**Figure 9.** *Molecular structure of norbormide.*

Norbormide [5-( $\alpha$ -hydroxy- $\alpha$ -2-pyridiylbenzyl)-7-( $\alpha$ -2pyridylbenzylidene)-5-norbornene-2,3-dicarboximide] (NRB) (Fig. 9), is a drug endowed with rat-selective toxic action. *In vitro* studies have demonstrated that the species-selective toxicity of NRB is due to an extensive and irreversible vasoconstriction of rat peripheral vessels.

NRB is a mixture of eight *endo*- and *exo*-stereoisomers, each of which is a racemate (see: Results, Fig. 19). It was synthesized for the first time by Mohrbacher using the reaction of 2-benzoylpyridine with cyclopentadienyl sodium in alcohol to give, under certain conditions,  $\alpha$ -phenyl- $\alpha$ -[6-phenyl-6-(2-pyridyl)-2-pyridinemethanol which then readily reacts with maleimide to give NRB (fig 10).

NRB melting point is 190-198° and solubility is 14 mg/L in ethanol, >150 mg/L in chloroform, 1 mg/L in diethyl ether, and > 26 mg/L in dimethylformamide. NRB is almost insoluble in water, is hydrolyzed in alkaline medium and is stable at room temperature.

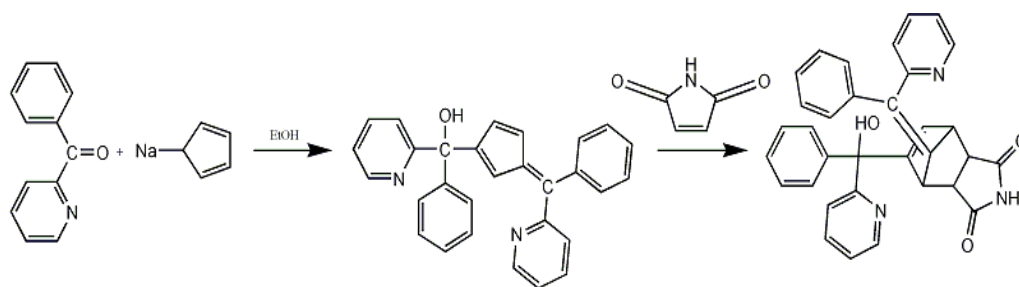


**Figure 10.** *Scheme of norbormide synthesis*

### 3.2. Pharmacological effects

NRB is the most selective vasoconstrictor so far known due to its property to exclusively constrict the peripheral arteries of the rat. This synthetic compound was introduced as a specific rat toxicant in 1964 (Roszkowsky *et al.*, 1964). Later, it was found that the eight racemic stereoisomers strongly differ in their vasoconstrictor activity and toxicity, thus indicating that NRB action is stereospecific. Indeed, only the *endo* isomers of NRB retain the rat-selective vasoconstrictor and toxicity activity elicited by mixture (Brimble *et al.*, 2004; Steel *et al.*, 2004; Poos *et al.*, 1966)

The rat-selective toxicity of NRB was described for the first time by Roszkowsky and colleagues in 1964 (Roszkowsky *et al.*, 1964). The acute toxic effects of this compound *in vivo* were studied and the doses of this agent needed to induce 50% lethality ( $LD_{50}$ ) were determined in four different strains of rats and in more than 30 other species, either mammalian (including primates), avian and fish (Tab 1). The data in table show that in rats the oral  $LD_{50}$  ranged between 5.3 and 52.0 mg/kg, depending on the strain of the rats used. In some strains of rats  $LD_{50}$  of NRB was as low as 0.64 mg/kg i.v. At much higher doses, this compound was lethal also in some of the other animal species. The oral  $LD_{50}$  in mouse, hamster, guinea pig and rabbit were 2250, 140, 620 and 1000 mg/kg respectively, while in other species NRB had no effects at doses of 1000 mg/kg or higher. The lethal effects of NRB were, therefore, highly selective for rats.

**Table 1. DL<sub>50</sub> values for norbormide in several animal species (Roszkowsky, 1965).**

Common name	Strain	Sex	N° Animals	DL <sub>50</sub> (mg/Kg)	Notes
Rat	Rattus norvegicus	M,F	70	10.15 (5.3-15)	<b>Oral DL<sub>50</sub></b>
Ox	Bos Taurus	M,F	2	>100	<b>No effect at 100</b>
Cat	Felis catus	M,F	6	>1000	<b>No effect at 1000</b>
Chicken	Gallus domesticus	M,F	20	>1000	<b>No effect at 1000</b>
Dog	Canis familiaris	M,F	6	>1000	<b>No effect at 1000*</b>
Fox	Vulpes vulpes	M,F	2	>1000	<b>No effect at 1000</b>
Goose	Branta Canadensis	M,F	4	>1000	<b>No effect at 1000</b>
Marmot	Citellus sp.	M,F	12	>1000	<b>No effect at 1000</b>
Guinea pig	Cavia porcellus	M,F	50	620 (530-711)**	
Horse	Equus caballus	M	1	>100	<b>No effect at 100</b>
Mink	Mustela vison	M,F	4	>1000	<b>¼ dead at 1000</b>
Monkey	Macaca mulatto	F	2	>1000	<b>No effect at 1000</b>
Mouse	Mus musculus	M	55	390 (291-523)**	<b>Intraperitoneal DL<sub>50</sub></b>
		F	44	2250 (1760-2880)**	<b>oral DL<sub>50</sub></b>
Nutria	Myocastor coypus	M	2	>1000	<b>No effect at 1000</b>
		F	5	>250<500	<b>2/2 dead at 1000; 1/1 dead at 500; 0/1 dead at 250 and 125</b>
Pigeon	Columba livia	M,F	6	>1000	<b>No effect at 1000</b>
Rabbit	Oryctolagus cuniculus	M,F	31	>1000	<b>No effect at 1000</b>
Sheep	Ovis aries	M,F	2	>1000	<b>No effect at 1000</b>
Squirrel	Sciurus vulgaris	M,F	4	>1000	<b>No effect at 1000</b>
Pig	Sus sp.	M,F	2	>1000	<b>No effect at 1000</b>

\* Light gastrointestinal hemorrhage of uncertain origin observed in 2/6 dogs

\*\* 95% confidence limits

Roszkowsky investigated the **cardiovascular effects** of this compound in rats. By intravascular administration to rats, NRB at sub-lethal doses increased blood pressure, produced marked bradycardia, arrhythmic episodes, and occasionally a brief apnea. All these effects were reversible. At lethal doses NRB produced always a profound and precipitous fall in blood pressure followed by cessation of respiration; the constriction of mesenteric and ear vessels became profound and irreversible. The NRB selective toxic effect was due to a generalized constriction of the peripheral arteries that led to a severe ischemic state in a number of vital organs and tissues with consequent failure of their function. A subsequent study confirmed Roszkowsky's findings in rats and demonstrated that the death of the animals was due to an acute heart failure (Roszkowsky *et al.*, 1965; Yelnosky and Lawlor, 1971; Bova *et al.*, 2001). The mechanism of NRB-induced toxicity at high concentrations in species other than rats was not established but it did not appear to involve vasoconstriction. It can be concluded that NRB, although it can be toxic in other species, causes rat-specific vasoconstriction, which is restricted to the peripheral arteries of the animal.

Recently, the vascular effect of NRB has been more extensively investigated and better characterized by using isolated artery rings and single freshly-prepared vascular smooth muscle cells from different vascular beds of rat and non rat species, including human one (Bova *et al.*, 1996; Fusi *et al.*, 2002; Bova *et al.*, 2001a). These studies showed that the effect on the vascular tissue interested directly smooth muscle cells. The surprising finding was that in all tested arteries from other species, as well as in aorta and extravascular smooth muscle, NRB exhibited vasorelaxant properties at concentrations that induced vasoconstriction in the rat peripheral arteries.

In the last years, several studies have been performed in the attempt to identify the mechanisms underlying NRB-induced vasoconstriction and vasorelaxation. Available evidence suggests that the vasoconstrictor effect may be mediated by the stimulation of the phospholipase C (PLC)- protein kinase C (PKC) signalling cascade with promotion of  $\text{Ca}^{2+}$  influx mainly *via* verapamil insensitive  $\text{Ca}^{2+}$  channels (Bova *et al.*, 2001a). The mechanism(s) involved in NRB-induced stimulation of PLC-PKC cascade is unknown; however, since this biochemical pathway is shared by most receptor-coupled vasoconstrictor agents, it has been hypothesized that NRB selective vasoconstriction could be due to its interaction



with a PLC-coupled receptor, uniquely expressed in the myocytes of the rat terminal arteries (Bova *et al.*, 2001a).

The mechanism involved in NRB-induced relaxation of rat aorta and non-rat arteries has not been elucidated. On the basis of indirect evidences, it was proposed that the drug could induce vasorelaxation by reducing  $\text{Ca}^{2+}$  channels activity (Bova *et al.*, 2001a). Such evidences came from patch-clamp studies performed on guinea pig ventricular myocytes, in which NRB was shown to reduce L-type  $\text{Ca}^{2+}$  current (Bova *et al.*, 1997), and from experiments carried out on guinea pig isolated hearts (Langendorff preparation) in which it caused functional and electrocardiographic modifications similar to those induced by the  $\text{Ca}^{2+}$  entry blocker verapamil (Bova *et al.*, 1997).

The species-specific and tissue-specific effect of NRB makes this drug unique in toxicology and potentially a very important tool in pharmacology because it indicates the existence of receptor-mediated species- and tissue-selective mechanisms that can be modulated by pharmacological agents. The NRB action is very intriguing and it could be very helpful to investigate selective drugs with tissue-specific action or new classes of species-specific toxicants.

### 3.3. Mitochondrial effects

A species-specific action of NRB has also been observed at the level of **mitochondrial function**. Patil and Radhakrishnamurty (1977) reported that low concentrations of NRB altered the ATPase activity of mitochondria isolated from rat liver while no changes were observed in mice. Induction of matrix swelling and decrease in both succinate- and ATP-driven  $\text{Ca}^{2+}$  uptake in rat liver mitochondria were also reported, but the mechanistic basis for these effects of NRB, and their relevance, remained unclear.

Recent studies demonstrated that these mitochondrial alterations could be traced to the opening of the inner membrane permeability transition pore (PTP) (Ricchelli *et al.*, 2005).

NRB did not affect the basic parameters that modulate the pore. In particular, the respiratory capacity and coupling efficiency of NRB-treated mitochondria were

adequate to sustain the proton electrochemical gradient; moreover, NRB did not affect  $\text{Ca}^{2+}$  uptake before the onset of the permeability transition, ruling out that the PTP opening was due to an alteration of  $\text{Ca}^{2+}$  transport. On the other hand, NRB induced rat-specific changes in the fluidity of the lipid interior of mitochondrial membranes, as revealed by fluorescence anisotropy of various reporter molecules. Such changes were accompanied by a higher sensitization of the PTP by the internal  $\text{Ca}^{2+}$  regulatory site. A correlation between changes in mitochondrial membrane fluidity and stimulation of PTP opening was supported by the results obtained with the other two tested animal species, mouse and guinea pig. The internal mitochondrial membrane regions of these species were insensitive to the perturbing effects of NRB, probably because in these species the drug was not able to cross the membrane barrier. These findings suggested the existence of a rat-specific mitochondrial surface transport system that allows the internalization of the drug across the membranes. This putative carrier could be absent in the latter species, or shielded from contact with the drug due to different membrane structural arrangements (Ricchelli *et al.*, 2005).

#### 4. AIM OF THE STUDY

It was recently demonstrated that the rat-selective toxicant norbormide (NRB) also induces rat-selective opening of the permeability transition pore (PTP) in isolated mitochondria.

a) The first aim of the present study was to investigate whether the species-specific PTP modulation and toxicity are causally linked, as suggested by the fact that both processes are specific to the rat. As reported in the Introduction, NRB is a mixture of *endo* and *exo* stereoisomers; however, only the *endo* forms are lethal to rats. Thus, we tested both *endo* and *exo* isomers to verify if: i) the PTP-regulatory activity by NRB is also stereospecific; ii) the NRB isomer activity is selective to rats. To address these questions, studies were carried out by following the  $\text{Ca}^{2+}$  retention capacity, the matrix swelling and the collapse of the membrane potential (as very sensitive methods to detect PTP opening) in isolated rat, mouse and guinea pig liver mitochondria.

b) The second aim of our research was to define the structural features of NRB responsible for PTP-activation. A series of NRB analogues derived from the “deconstruction” of the parent molecule at three key sites (substituents at C-5, C-7 and the imide unit) was evaluated in order to assess the most active substructural moiety.

c) Finally, the mechanism of NRB action was further investigated by carrying out studies with cationic derivatives of the drug, which should accumulate in mitochondria driven by the inside-negative membrane potential. The availability of active cationic derivatives which accumulate in the matrix could provide a unique opportunity to test whether the lack of effects of NRB in mouse and guinea pig mitochondria depends on species-related differences in PTP structure or rather in drug transport.

Our results show that: (a) NRB isomers affect PTP in a rat-selective fashion; however, no relevant differences between lethal and non-lethal forms are observed suggesting that drug regulation of PTP-activity and lethality in rats are unrelated phenomena; (b) The (phenylvinyl)pyridine moiety represents the key element conferring to NRB the PTP-activating effect; (c) Cationic derivatives of rat-active

compounds accumulate in the matrix *via* the membrane potential and activate the PTP also in mouse and guinea pig mitochondria. These findings suggest that the NRB-sensitive PTP-target is present in all species examined, and is presumably located on the matrix side. The species-selectivity may depend on the unique properties of a transport system allowing drug internalisation in rat mitochondria.

## 5. MATERIALS AND METHODS

### 5.1. Materials

Norbormide was a kind gift of I.N.D.I.A. Industria Chimica, Padova (Italy). 1,6-diphenyl-1,3,5-hexatriene (DPH), 1-(4-trimethylammoniumphenyl)-6-phenyl-1,3,5-hexatriene p-toluene sulfonate (TMA- DPH) and pyronine G (Pyr G) were products of Sigma. Calcium Green-5N was purchased from Molecular Probes, Invitrogen. Other chemicals used were of analytical reagent grade.

All isolated NRB isomers and the following NRB analogues were prepared by David Rennison, Olivia Laita, and Jessica Stäb in the laboratories of the University of Auckland, New Zealand, as previously described (Brimble *et al.*, 2004; Steel *et al.*, 2004; Rennison *et al.*, 2007):

*endo*-7-( $\alpha$ -2-pyridylbenzylidene)-5-norbornene-2,3-dicarboximide (DR085), 2-(1-phenylvinyl)pyridine (DR166), 2-(1-phenyl-2-ethanol)pyridine (DR282), 5-( $\alpha$ -hydroxy- $\alpha$ -2-pyridylbenzyl)-7-( $\alpha$ -phenylbenzylidene)-5-norbornene-2,3-dicarboximide (DR488), 5-( $\alpha$ -hydroxy- $\alpha$ -2-pyridylbenzyl)-5-norbornene-2,3-dicarboximide (DR496), and (unpublished data):

norbornene-2,3-dicarboximide (DR067), *endo*-7-( $\alpha$ -2-phenylbenzylidene)-5-norbornene-2,3-dicarboximide (DR068), 2-benzylpyridine (DR303) and 2-(1-phenylethyl)pyridine (DR322) as well as the cationic derivatives: *N*-ethyl-2-(1-phenylvinyl)pyridinium trifluoromethanesulfonate (DR380), 5-( $\alpha$ -hydroxy- $\alpha$ -2-pyridylbenzyl)-7-(*N*-pivaloyloxymethyl- $\alpha$ -2-pyridiniumbenzylidene)-5-norbornene-2,3-dicarboximide iodide (OL14), *N*-pivaloyloxymethyl-2-(1-phenylvinyl) pyridinium iodide (JS023) and *N*-pivaloyloxymethyl-2-(1-phenyl-2-ethanol)pyridinium iodide (DR656)

1,1-Diphenylethylene (DR598) was obtained commercially (Aldrich).

### 5.2. Methods

#### 5.2.1. Isolation of mitochondria and determination of mitochondrial proteins.

Albino Wistar rats, CD1 mice and albino guinea pigs (from Charles River, Italy)

were starved overnight (this step is necessary to decrease the content of fat and glycogen in the liver); then, they were sacrificed in accordance with institutional guidelines and the aims of the experiment. The liver ( $\cong$  20-30 gr) was removed and immersed immediately in ice-cold Tris/HCl buffer pH 7.4 containing 0.25 M sucrose and 0.1 mM EGTA (Isolation Buffer-IB-); then, it was cut into small pieces with scissors and washed several times by replacing the ice-cold IB with fresh ice-cold buffer, in order to remove as much blood as possible.

The mitochondria preparation follows three simple steps: (i) rupturing of cells by mechanical means, (ii) differential centrifugation at low speed to remove debris and extremely large cellular organelles (SPIN 1), and (iii) centrifugation at a higher speed to isolate and collect mitochondria (SPIN 2).

**1. RUPTURE:** The minced tissue suspended in IB (8 ml per gram of liver) was homogenized in pre-chilled Potter homogenizer with pestle. To rupture the cells, a number of strokes was performed.

**2. SPIN 1:** The homogenate was centrifuged in a Beckman GS-15R (rotor's model FO850) centrifuge at 4°C for 10 minutes at 600g to remove cells, nuclei and tissue fragments. The pellet was discarded whereas the supernatant was saved.

**3. SPIN 2:** The supernatant was transferred into two tubes, each of which filled to 2.0 ml with IB, and centrifuged at 6800g for 10 min at 4 °C. Each pellet was washed by resuspending in 1.0 ml of IB, then centrifuged at 12,000 g for 5 min at 4 °C. Finally, combined pellets were resuspended in 1 ml of IB to give a protein concentration of 80-100 mg/ml, as measured using the biuret method.

In the protein determination with biuret, 20  $\mu$ l of mitochondria were suspended in 1ml of H<sub>2</sub>O + 0,5ml DOC (deoxycholic acid) 1% + 1,5ml biuret. The standard solution was prepared without mitochondria. Both solutions were put in a thermostated bath (100 °C) for 1 minute and then cooled with water. The protein concentration was measured at 540 nm using a spectrophotometer Perkin Elmer UV/VIS Lambda 2. The absorption value at 540 nm was related to the total protein concentration (mg/ml) by a standard calibration curve.

### **5.2.2. Mitochondrial oxygen consumption (RCR test)**

The quality of isolated mitochondria was estimated by measuring the Respiratory

## Control Ratio (RCR).

One of the keystones of the chemiosmotic theory of energy transduction is impermeability of the inner mitochondrial membrane to protons. Oxidation of substrates results in extrusion of protons from the mitochondrial matrix to generate the mitochondrial membrane potential. High membrane potential suppresses further extrusion of protons and therefore inhibits respiration. Under resting conditions, the rate of respiration of mitochondria is quite low and determined by a passive leakage of protons into the matrix space. Phosphorylation of ADP requires translocation of protons into the matrix through mitochondrial ATP synthase. This results in a decrease in membrane potential that stimulates respiration. Comparison of the rates of respiration in the resting state and during phosphorylation of ADP is a useful measure of the efficiency of mitochondrial functioning. The most reliable and widely used criterion of the quality of a mitochondrial preparation is the respiratory control ratio (RCR). RCR is defined as the rate of respiration (oxygen consumption) in the presence of ADP (phosphorylating respiration, state 3) divided by the rate obtained in the absence of ADP, state 4.

Mitochondrial oxygen consumption was measured polarographically in a thermostated ( $T = 25\text{ }^{\circ}\text{C}$ ), water-jacketed vessel, using a Clark-type oxygen electrode connected to a recorder:

- 2 ml of incubation buffer (Tris/buffer containing 100 mM sucrose, 50 mM KCl, 10 mM  $\text{KH}_2\text{PO}_4$ , 2mM  $\text{MgCl}_2$ , 1mM EDTA pH 7.4) for testing mitochondrial quality were put into the sample chamber of the oxygen monitor and conditions to constant stirring were setted (Fig. 11). After some min stabilization observed by recorder trace, an aliquot of mitochondrial suspension was added for a final concentration of 0.5 mg/ml mitochondrial protein. Rotenone (to block oxidation of the endogeneous substrates) to a final concentration of 2.0  $\mu\text{M}$  and sodium succinate (energizing substrate) for a final concentration of 5 mM were also added. As shown in the figure, mitochondria started to consume oxygen. The slope of the curve shows the rate of respiration.

- After stabilization of respiration, ADP (final concentration 0.3 mM) was added. The rate of respiration greatly increased (state 3) with subsequent restoration of the initial rate of respiration (state 4) when all added ADP was phosphorylated.
- The rate of respiration was calculated from the recorder trace as the amount of oxygen consumed in 1 min, assuming that at room temperature and normal atmospheric pressure the concentration of oxygen in the incubation buffer is 240  $\mu\text{M}$ . RCR was calculated by dividing the state 3 respiration rate by the state 4 respiration rate.

Mitochondria with a RCR  $\geq 3$  were acceptable for use in the experiments.

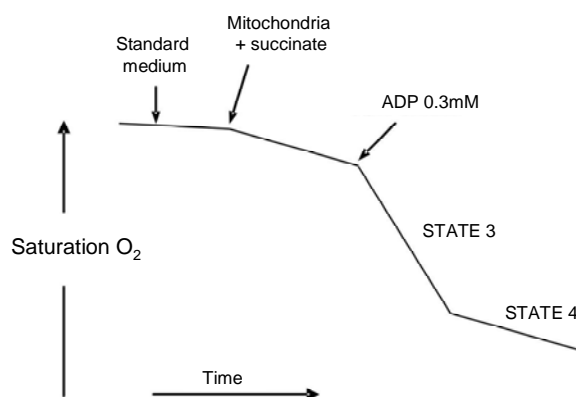


**Figure 11. Experimental trace of oxygen consumption by mitochondria**

### 5.2.3. Mitochondrial permeability transition (PT). Matrix swelling as measured by *light-scattering (LS)* changes.

Mitochondrial volume homeostasis is a housekeeping cellular function essential for maintaining the structural integrity of the organelle. Changes in mitochondrial volume due to a variety of stimuli have been associated with a wide range of important biological functions and pathologies. Mitochondrial matrix volume is controlled by osmotic balance between cytosol and mitochondria. Any dysbalance in the fluxes of the main intracellular ions (e.g. potassium) will thus affect the osmotic balance between cytosol and the matrix and promote the water movement between these two compartments. It has been hypothesized, for ex., that activity of potassium efflux pathways exceeds the potassium influx in functioning mitochondria and that potassium concentration in matrix could be actually lower than in cytoplasm. This hypothesis provides a clear-cut explanation for the



mitochondrial swelling observed after mitochondrial depolarization, mitochondrial calcium overload, or opening of permeability transition pore. It should also be noted that the rate of water flux into or out of the mitochondrion is determined not only by the osmotic gradient that acts as the driving force for water transport but also by the water permeability of the inner membrane. Recent data suggest that the mitochondrial inner membrane has also specific water channels, aquaporins, which facilitate water movement between cytoplasm and matrix.

Mitochondria swelling can be easily determined by light scattering (LS) measurements. Actually, when mitochondria swell their refraction index decreases, thereby decreasing the intensity of scattered light. The correlation between the amount of light scattered by a mitochondrial suspension and the volume of mitochondrial matrix was extensively exploited for qualitative studies of solute transport across the inner membrane.

Mitochondrial volume changes during the PT are associated with a large decrease of LS intensity. This decrease was followed at 540 nm, using a Perkin-Elmer LS-50B spectrophotofluorimeter equipped with magnetic stirring and thermostatic control ( $T = 25^{\circ}\text{C}$ ) for mitochondria suspended in a medium containing 200 mM sucrose, 20  $\mu\text{M}$  EGTA, 10 mM Tris-Mops, 5 mM succinate, 2  $\mu\text{M}$  rotenone, 1 mM  $\text{KH}_2\text{PO}_4$ , 3  $\mu\text{g/ml}$  oligomycin, pH 7.4 (Petronilli *et al.*, 1993) (standard medium).  $\text{Ca}^{2+}$  was used as PT inducer. Due to the optical arrangement of the instrument, LS was measured at  $90^{\circ}$  from the incident light.

#### **5.2.4. Mitochondrial permeability transition (PT). Release of matrix $\text{Ca}^{2+}$ as measured by the calcium retention capacity (CRC) with a $\text{Ca}^{2+}$ fluorescent probe, Calcium Green-5N.**

The calcium retention capacity (CRC) is the amount of calcium that mitochondria can accumulate and retain before opening of the PT pore. Pore opening causes the release of calcium accumulated into the mitochondrial matrix into the external medium. Thus, it is possible to investigate the cycles of  $\text{Ca}^{2+}$  uptake by and release from mitochondria by monitoring the fluxes of extramitochondrial  $\text{Ca}^{2+}$ . Extramitochondrial  $\text{Ca}^{2+}$  was measured fluorimetrically using Calcium Green-5N (Fig. 12), a membrane-impermeant probe that is poorly fluorescent *per se*. This

$\text{Ca}^{2+}$ -indicator exhibits a drastic increase in fluorescence emission intensity upon  $\text{Ca}^{2+}$  binding (excitation-emission  $\lambda$ : 480-530 nm). All measurements were carried out in the standard medium. A detailed description of this methodology is reported in : Results, to explain Fig. 18.

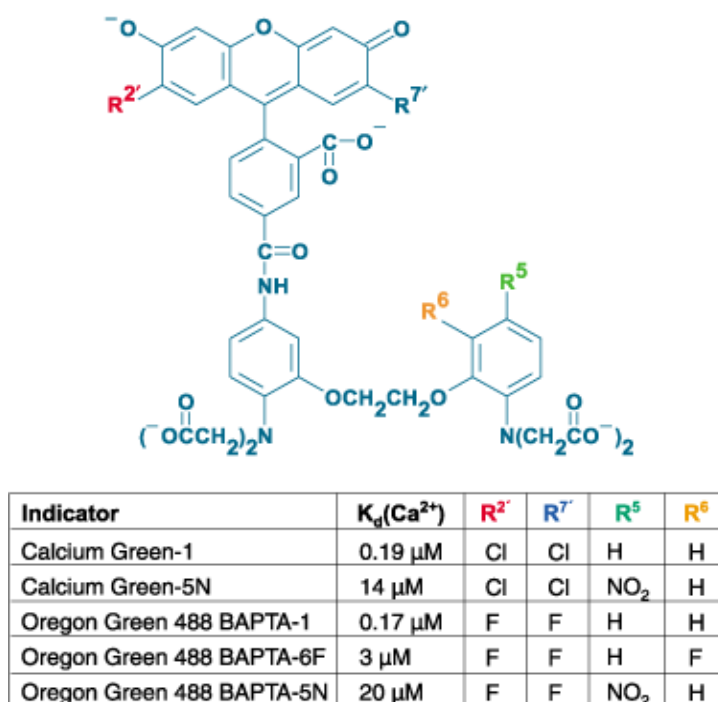


**Figure 12.** Chemical structure of different  $\text{Ca}^{2+}$ -indicators, including Calcium Green-5N.

#### 5.2.5. Mitochondrial permeability transition (PT). Collapse of the membrane potential as measured by the fluorescence changes of pyronin G, a probe of membrane potential.

The PT process is accompanied by collapse of the mitochondrial membrane potential ( $\Delta\psi_m$ ).  $\Delta\psi_m$  changes were followed by the changes in the fluorescence of the cationic dye, pyronin G (Pyr G) (Tomov, 1986) (Fig. 13). In the Pyr G molecule there are many apolar sections (aromatic nuclei, methyl groups-see figure below-) that confer to the pyronin cation some degree of lipophilicity and allows it to cross the mitochondrial membranes.

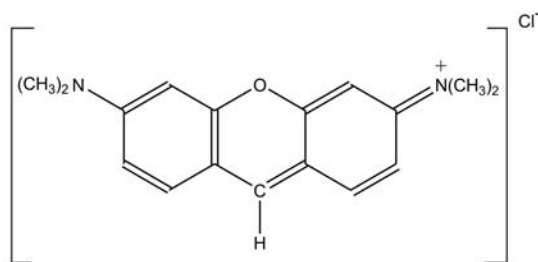


**Figure 13. Chemical structure of Pyr G**

In this set of experiments the mitochondrial suspensions were loaded with 3  $\mu\text{M}$  Pyr G; then, the Pyr G fluorescence emission intensity was recorded at  $\lambda = 580$  nm (excitation  $\lambda = 520$  nm).

At the beginning of the recording the oxidation of endogenous substrates was blocked by rotenone, mitochondria were in de-energized state and the membrane potential  $\Delta\psi_m$  was equal to 0. Under these experimental conditions, the Pyr G fluorescence intensity was high (see Fig. 14).

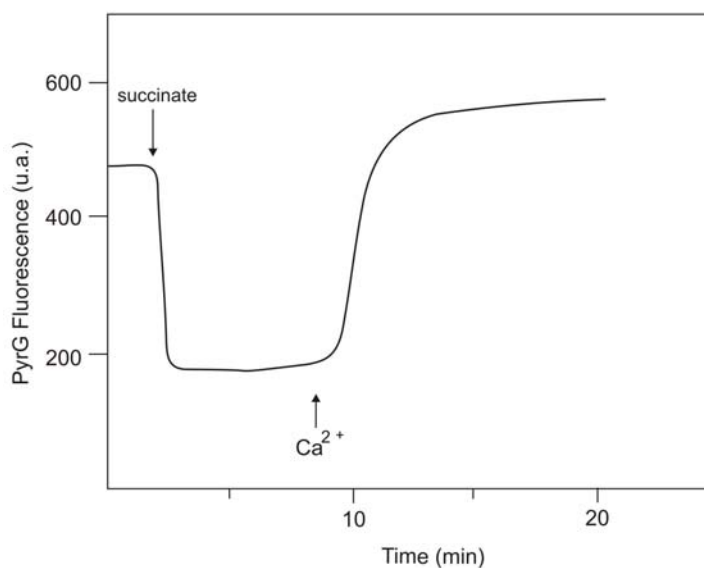


**Figure 14. Dependence of the fluorescence on the membrane potential of the mitochondria.**

When the respiratory substrate, succinate, was added, the mitochondria passed into energized state and  $\Delta\psi_m \neq 0$  (up to  $\sim -200\text{mV}$ ). Increase of the membrane potential of mitochondria caused a decrease of Pyr G fluorescence.

When excess  $\text{Ca}^{2+}$ , for ex., was added to induce PTP opening, there was dissipation of the electrochemical gradient of the membrane, mitochondria returned in a de-energized state and  $\Delta\psi_m = 0$ .

The properties of Pyr G make it possible to explain the mechanism of the influence of the membrane potential of the mitochondria on the fluorescence of the dye. When  $\Delta\psi_m=0$ , Pyr G is evenly distributed between the medium and the inner space (matrix) of the mitochondria. As the concentration is low, the dye is entirely in fluorescing monomeric form and the intensity of the fluorescence is maximal. When  $\Delta\psi_m \neq 0$ , the pyronin cations are redistributed according to the Nernst's equation and the concentration of dye in the matrix increases by several orders. The high Pyr G concentration in the mitochondria leads to the formation of fluorimetrically silent aggregates. The average concentration of fluorescing monomers in the suspension decreases and this results in reduced fluorescence intensity.

#### **5.2.6. Fluorescence anisotropy measurements**

##### *An introduction to fluorescence polarization/anisotropy*

It is possible to get information about the size and shape of protein molecules, as well as the structure of lipid membranes by studying their Brownian motion. Such motion involves not only the translation of the molecules but also their rotational movements. When the molecules are fluorescent, the rotational motion can be easily investigated by following the polarization (or anisotropy) properties of the emitted radiation. Non-fluorescing structures can be labelled by a fluorescent dye.

The theoretical basis of the fluorescence polarization (or anisotropy) is briefly described as follows:

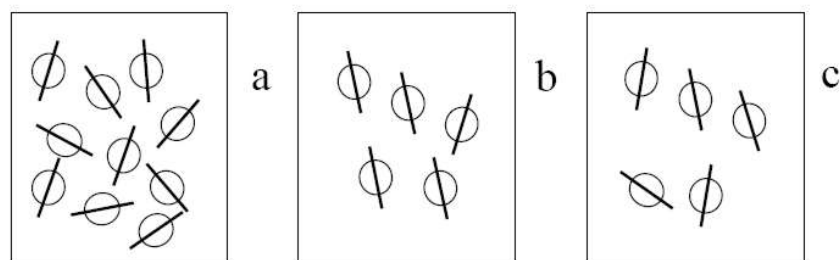


**Figure 15. Isotropic and anisotropic distribution of fluorescent molecules**

Imagine first of all a set of fluorescent molecules in solution and suppose that a given direction is rigidly bound to the molecules. At any instant, all possible directions are equally represented (**isotropic distribution** of the fluorophores), and the molecules are thus randomly disposed, as in Figure 15(a). If now the solution is illuminated with a beam of plane polarized light, we will observe a **photoselection of molecules**, that is, only those molecules oriented around a particular direction will be excited. It is known that the absorption and emission of light by organic molecules is connected with fixed directions of the molecules, the so-called oscillators of absorption and emission, and that the molecules will have a good chance of absorbing the exciting light only if the direction of their absorption oscillator is parallel, or nearly so, to the plane of vibration of the exciting wave. Thus, the excited molecules form nearly a state like (b) (highly ordered, **anisotropic distribution** of the fluorophores).

Each photoselected molecule then emits a polarized radiation in a plane parallel to its emission oscillator. If the time interval between absorption and emission is long, the molecules will re-orientate randomly, the photoselection will be lost and no polarization will be observed; but if the time interval is short enough they may be observed in a state represented by (c) where randomization is not yet complete, that is, the orientation prevailing at the time of excitation is partially preserved. In this case, the fluorescent light will show partial polarization.

Thus, the degree of fluorescence polarization depends only on two factors: the interval between excitation and emission (**lifetime of the excited state,  $\tau$** ) and the speed of rotation of the molecule in solution (**rotational relaxation time**). Generally, fluorescence polarization is not observed in aqueous solution and at room temperature because most of the molecules exhibit relaxation time shorter than  $\tau$ . On the contrary, a fluorophor incorporated into proteins or lipid bilayers

undergoes rotational constrictions due to the binding and its relaxation time will coincide with that much longer of the incorporating macromolecular structure. Consequently, the emitted fluorescence will result partially polarized.

The polarization also increases at increasing medium viscosity and at decreasing temperatures, due to slowing of Brownian motions.

Based on the photoselection characteristics, the fluorescence emission is also proportional to the degree of order (**anisotropy**), then to the rigidity, of the system under examination.

#### *Fluorescence polarization/anisotropy detection*

The device we used for fluorescence polarization detection is described schematically in Figure 16:

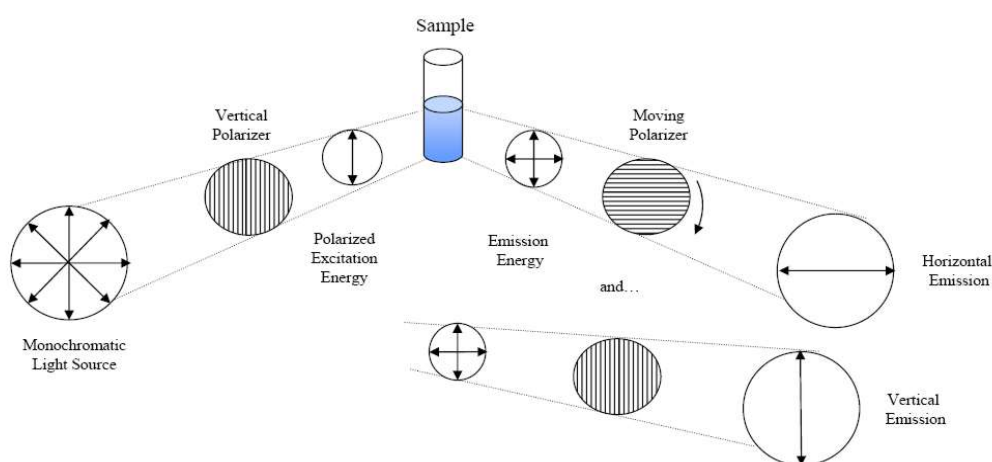


**Figure 16. Schematic representation of fluorescence polarization detection.**

Unpolarized monochromatic light passes through a polarizing filter. Polarized light vibrating in a plane vertical (V) to the propagation plane (H) of the radiation is selected to excite fluorescent molecules in the sample cuvette. Only those molecules that are oriented properly in the vertically polarized plane absorb light, become excited, and subsequently emit light. The intensity of emitted light is collected through a movable polarizing filter in both the vertical ( $I_{VV}$ , maximal polarization) and horizontal ( $I_{VH}$ , minimal polarization) planes (the degree of movement of emission intensity from vertical to horizontal plane is related to the mobility of the fluorescently labelled molecule).

Anisotropy (r) is then calculated according to the equation:

$$r = (I_{VV} - GI_{VH}) / (I_{VV} + 2GI_{VH})$$

$G = I_{HV} / I_{HH}$  is the correction factor for instrumental artefacts, calculated by using horizontally (H) polarized exciting light. Correction must be introduced since instrumental elements do not equally reflect the perpendicular and parallel components of the emitted light.

Clearly, the anisotropy value, r, being a ratio of light intensities, is a dimensionless entity.

Fluorescence anisotropy measurements have been performed with a Perkin-Elmer LS 50 spectrophotofluorimeter, equipped with a pulsed xenon lamp and polarizers, and connected to a computer that automatically calculates and combines the various components of the anisotropy. The optical arrangement of the instrument was at 90 °(between incident and emitted radiation).

#### *Experimental application*

The fluorescence polarization is a powerful tool for studying molecular interactions by monitoring changes in the movements of fluorescently-labelled or inherently fluorescent molecules. It offers numerous advantages over more conventional methods, such as high sensitivity, prompt interpretation of the data, low limit of detection in the sub-nanomolar range, “real-time” measurements in kinetic assays and insensitivity to variations in concentration.

In this work, fluorescence polarization has been used to investigate the changes in the dynamic properties of mitochondrial membranes induced by NRB and various NRB derivatives. Despite the series of important advantages over, for ex., NMR and EPR techniques, the resolution of fluorescence polarization applied to a complex system such as mitochondria is limited since the districts of the biological membranes are highly heterogeneous. In actual fact, these molecular assemblies are characterized by the coexistence of structures with highly restricted mobility (“solid” domains) and components having great rotational freedom (“fluid” domains). Thus, in the common steady-state approach the results will be an average of different structural situations. These limitations, however, are shared by other biophysical methods. The interpretation of the data can be

facilitated using different membrane-fluorescent probes that are endowed with different hydro/lipophilicity properties and partition in specific membrane regions (Szöllösi, 1994).

The fluorescent probes used in this work are 6-phenyl-1,3,5-hexatriene (DPH) and 1-(4-trimethylammoniumphenyl)-6-phenyl-1,3,5-hexatriene p-toluene sulfonate (TMA-DPH). DPH is typically used to sense fluidity changes of the membrane hydrophobic lipid core (in particular between C-10 and C-12) and TMA-DPH to sense fluidity changes of the polar heads/lipid backbone interface regions (Figure 17). The latter lipid domains should mainly reside in the matrix-exposed leaflet of the inner membrane bilayer since the cationic TMA-DPH preferentially accumulates into the matrix driven by the inside-negative membrane potential (see: Results).

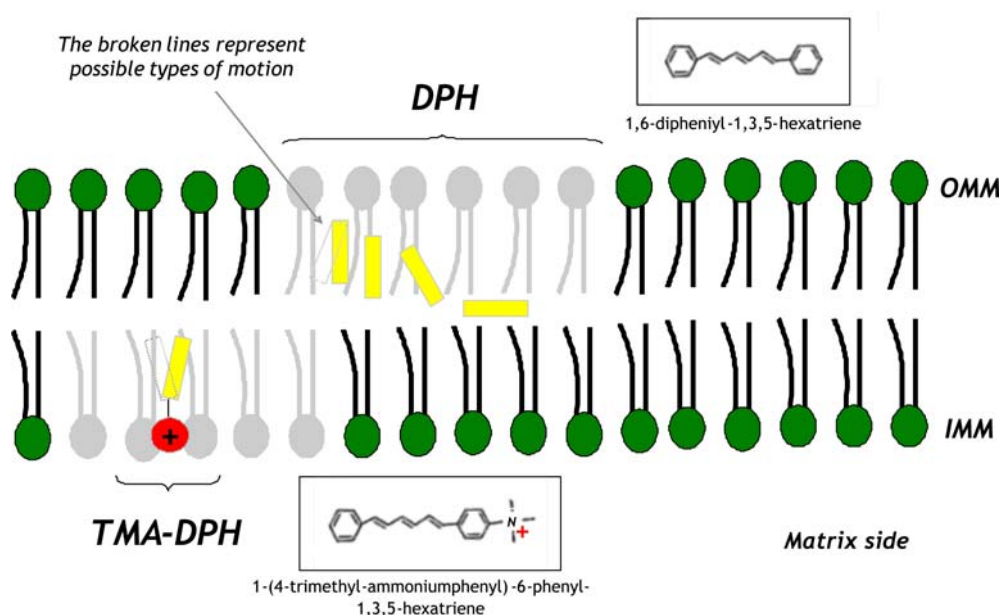


**Figure. 17. Schematic diagram of proposed locations in the mitochondrial lipid bilayer of the fluorescent probes DPH and TMA-DPH (from: Szöllösi, 1994).**

DPH- and TMA-DPH-labelled mitochondria were prepared by treating mitochondrial suspensions (20 mg/ml) with 300  $\mu$ M probe. After 20 min (DPH) or 5 min (TMA-DPH) incubation under continuous stirring at  $T = 25^\circ\text{C}$ , the mitochondrial suspensions were diluted to 0.2 mg/ml for anisotropy measurements.



The fluorescence anisotropy ( $r$ ) was collected at 340 nm ( $\lambda_{\text{em}} = 460$  nm) (for DPH) and 360 nm ( $\lambda_{\text{em}} = 430$  nm) (for TMA-DPH) by calculating the  $I_{\text{VV}}$  and  $I_{\text{VH}}$ , i.e. the fluorescence intensities polarized parallel and perpendicular to the vertical plane of polarization of the excitation beam respectively (see above).



## 6. RESULTS

### 6.1. Species-specific modulation of the mitochondrial PT by NRB

We studied the effect of NRB on the PT of mitochondria isolated from liver of different animal species (rat, mouse and guinea pig) using  $\text{Ca}^{2+}$  as PT inducer. We first investigated the mitochondrial  $\text{Ca}^{2+}$  overloading and the subsequent pore opening following two parameters, the *calcium retention capacity (CRC)* of mitochondria and the *matrix swelling*. As explained in Materials and Methods, CRC is the quantity of  $\text{Ca}^{2+}$  accumulated and retained by mitochondria before the occurrence of the PT; after pore opening, matrix  $\text{Ca}^{2+}$  is released into the external medium. The extramitochondrial  $\text{Ca}^{2+}$  was measured fluorimetrically using Calcium Green 5N, which exhibits an increase in fluorescence emission intensity upon  $\text{Ca}^{2+}$  binding. The mitochondrial swelling, due to the matrix permeation to external solutes, was detected as the decrease in the light scattering of the mitochondrial suspension at 540 nm.

In the experiments illustrated in Fig. 18 rat liver mitochondria were loaded with a train of 20  $\mu\text{M}$   $\text{Ca}^{2+}$  pulses at 1-min intervals. Each  $\text{Ca}^{2+}$  addition gave rise to rapid increases of the Calcium Green-5N fluorescence, followed by a return to the original steady-state value as  $\text{Ca}^{2+}$  was taken up by mitochondria. When the loading threshold of about 120 nmol of  $\text{Ca}^{2+}$ /mg protein was reached, net release of  $\text{Ca}^{2+}$  into the medium was observed (panel A, trace a). This fast process of  $\text{Ca}^{2+}$  release was due to the opening of the PTP because (i) it was accompanied by swelling (panel B, trace a); and (ii) the  $\text{Ca}^{2+}$  threshold was drastically increased in the presence of CsA (not shown). Incubation with 50  $\mu\text{M}$  NRB for 5 min (incubation time at which the maximal effect was observed, Ricchelli et al., 2005) decreased the  $\text{Ca}^{2+}$  load required for PTP opening to 60 nmol of  $\text{Ca}^{2+}$ /mg protein without affecting the rate of  $\text{Ca}^{2+}$  uptake (panels A and B, traces b).

In contrast to rat liver mitochondria, NRB did not influence the CRC of mouse (and guinea pig; not shown) liver mitochondria. Indeed, the experiments illustrated in Fig. 18 show that  $\text{Ca}^{2+}$  release from mouse mitochondria (panel C) occurred after mitochondrial loading with six pulses of 30  $\mu\text{M}$   $\text{Ca}^{2+}$  at 1.5-min

intervals, both in the absence (trace a) and the presence (trace b) of 50  $\mu\text{M}$  NRB. In both cases, inhibition by 1  $\mu\text{M}$  CsA indicated that  $\text{Ca}^{2+}$  release was PTP-dependent. Consistently, onset of PTP-dependent mitochondrial swelling (panel D, trace a) was only negligibly affected by NRB (trace b )

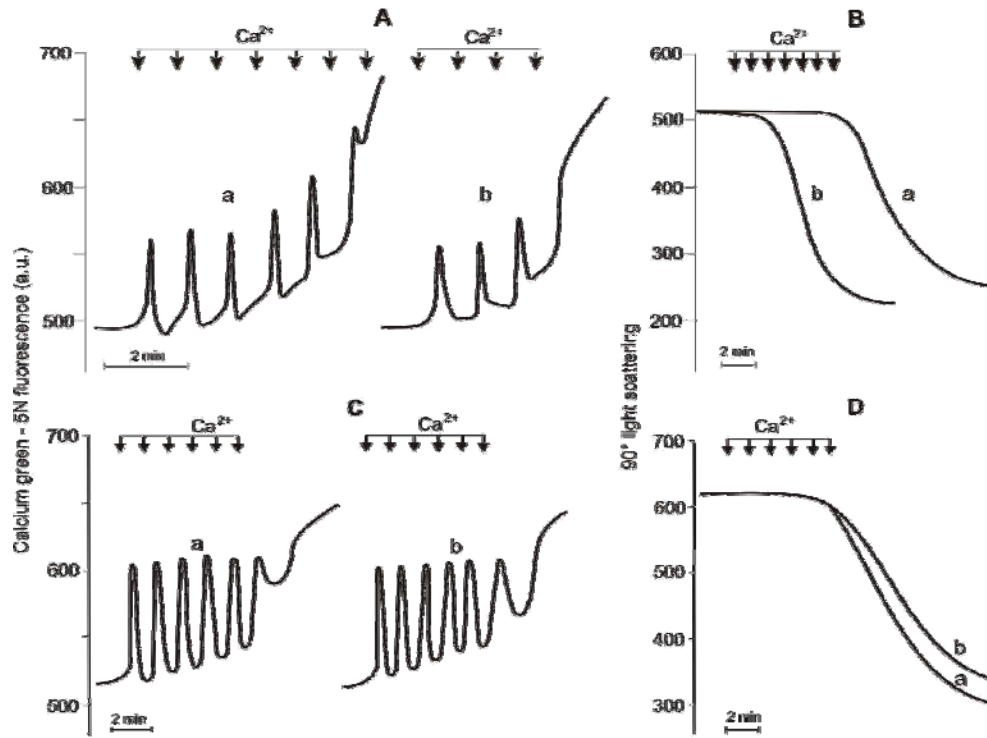


**Figure 18. Effect of NRB on the CRC of rat and mouse liver mitochondria.** The experiments were started by the addition of 1mg/ml mitochondria (not shown) to the standard incubation medium. (A, B) Rat liver mitochondria in the absence (traces a) or the presence (traces b) of 50  $\mu\text{M}$  NRB were loaded with a train of 20  $\mu\text{M}$   $\text{Ca}^{2+}$  pulses at 1-min intervals. In the experiment of traces b, mitochondria were pre-incubated for 5 min with NRB before addition of  $\text{Ca}^{2+}$ . (A) Extramitochondrial  $\text{Ca}^{2+}$  was monitored as the fluorescence emission of 0.5  $\mu\text{M}$  Calcium Green-5N ( $\lambda_{\text{excitation}} = 480 \text{ nm}$ ;  $\lambda_{\text{emission}} = 530 \text{ nm}$ ). (B) Mitochondrial volume changes were measured from the 90° light scattering changes at 540 nm. (C, D) The experiments with mouse liver mitochondria were performed as described above except that  $\text{Ca}^{2+}$  pulses of 30  $\mu\text{M}$  were added at 1.5-min intervals.

Experiments were performed also with heart and kidney mitochondria of the three species. The results were identical to those obtained with liver mitochondria, thus confirming that NRB-stimulated PTP opening was specific to rat; on the other

hand, the lack of activity of the drug in guinea pig and mouse mitochondria indicated that the process was not tissue-specific.

## 6.2. Correlation between vasoconstrictor activity (toxic effect) of NRB and regulation of mitochondrial PT.

NRB is a mixture of eight possible diastereoisomers each of which is a racemate (see the configurations below, Fig. 19). Since the S and U isomers are present in trace amounts, only the six most abundant isomers (V, Y, W, R, T, X) were tested for their PT-inducing activity on isolated mitochondria. Among them, only the *endo*- isomers V, Y, and W induce vasoconstriction and death in rats whereas the *exo*-forms R, T and X are ineffective (Brimble *et al.*, 2004; Steel *et al.*, 2004; Poos *et al.*, 1966).

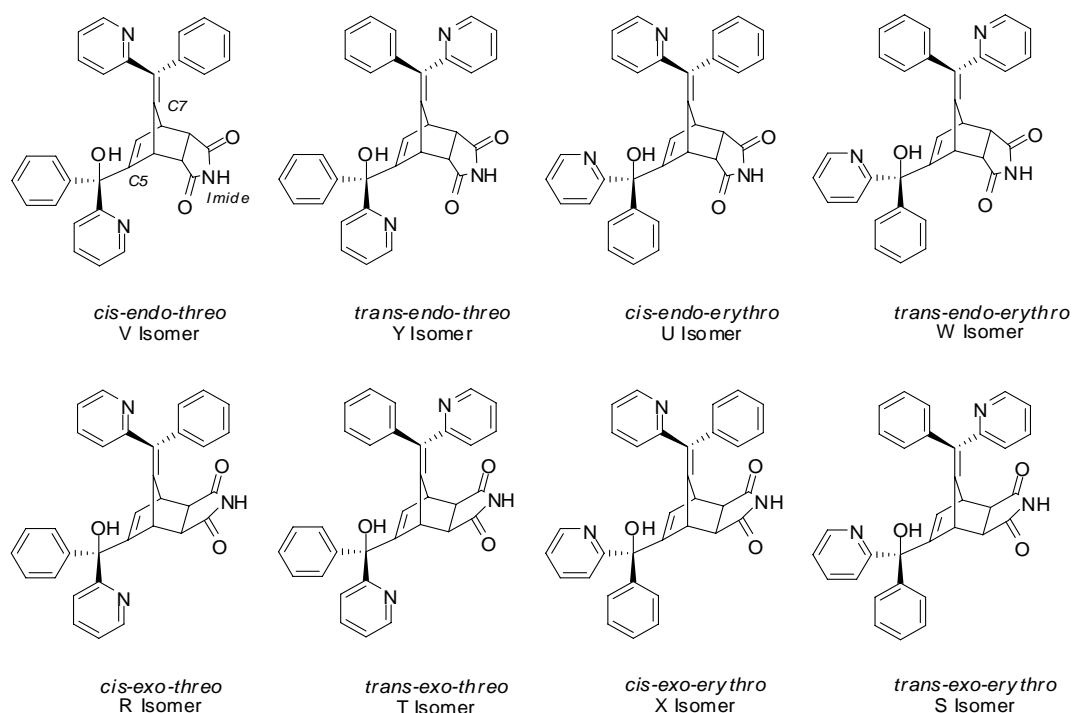


**Figure 19. NRB isomers**

PTP activation was tested by measuring the CRC of mitochondria after 5 min incubation with the different NRB isomers.

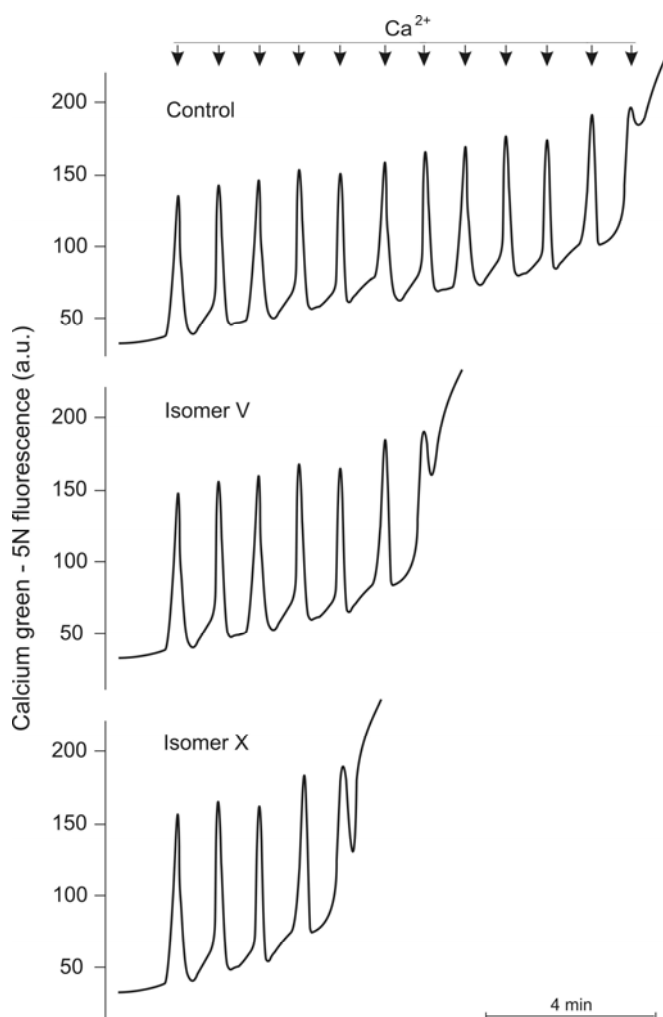


**Figure 20. Effects of the isomers X and V of NRB on the CRC of rat liver mitochondria.** The experiments were started by the addition of 1mg/ml mitochondria (not shown) to the standard incubation medium. Rat liver mitochondria were loaded with a train of 10  $\mu\text{M}$   $\text{Ca}^{2+}$  pulses at 1-min intervals. Mitochondria were pre-incubated for 5 min without (control) or with 50  $\mu\text{M}$  X or V before addition of  $\text{Ca}^{2+}$ . Extramitochondrial  $\text{Ca}^{2+}$  was monitored as the fluorescence emission intensity of 0.5  $\mu\text{M}$  Calcium Green-5N ( $\lambda_{\text{excitation}} = 480 \text{ nm}$ ;  $\lambda_{\text{emission}} = 530 \text{ nm}$ )

Fig. 20 shows the effects of 50  $\mu\text{M}$  isomer V and X (as representative of the lethal and non lethal NRB form, respectively) on the CRC of rat liver mitochondria. Incubation of mitochondria with isomers V and X for 5 min decreased the  $\text{Ca}^{2+}$  load required for PTP opening from 120 (control) to 70 and 50 nmol of  $\text{Ca}^{2+}$ /mg protein, respectively. In all cases, the addition of 1  $\mu\text{M}$  cyclosporin A doubled the CRC, indicating that  $\text{Ca}^{2+}$  release was due to opening of the PTP (data not shown). Dose-response tests indicated that all NRB isomers decreased the CRC of

rat mitochondria in the concentration range 5-100  $\mu\text{M}$ , the maximal effect being reached at approximately 40  $\mu\text{M}$  (data not shown).

Fig. 21 compares the effects of low (10  $\mu\text{M}$ ) and high (50  $\mu\text{M}$ ) concentrations of the NRB mixture and of the individual isomers on the CRC in rat, mouse and guinea pig mitochondria.

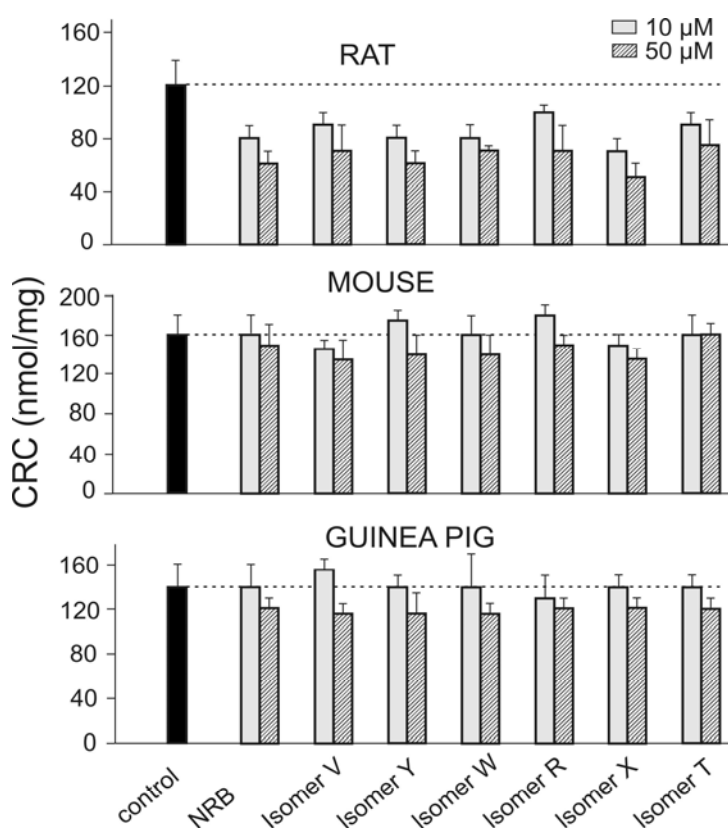


**Figure 21.** CRC of rat, mouse and guinea pig liver mitochondria in the presence of the NRB isomers V, Y, W, R, X, T at 10 and 50  $\mu\text{M}$ . The CRC was calculated according to the experimental procedure described in the legends to Fig. 18 and 20. Data are expressed as mean ( $\pm$  SD) of three independent determinations. Statistical analysis indicated that the data for rat mitochondria incubated with NRB and NRB isomers are significantly different from those of the controls (unpaired *t*-test,  $P < 0.01$ ).

From the results of Figs. 20 and 21 it is clear that all isomers were rat-selective in inducing the mitochondrial PT, and all were effective at relatively low concentrations. Importantly, no significant difference could be detected between toxic (V, Y, W) and non toxic (R, X, T) isomers.

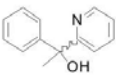
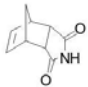
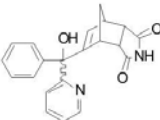
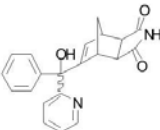
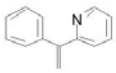
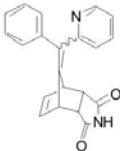
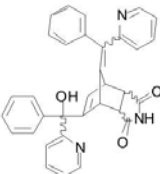
### 6.3. “The active core” of NRB molecule

In order to better define the key structural features of NRB responsible for PTP activation in rat mitochondria, we evaluated several related analogues, synthesized in the laboratories of the University of Auckland, New Zealand, on the basis of a selected “deconstruction” of the parent molecule at the three key sites (C-5, C-7 and the imide group) (Table 2). Table 2 also shows the structure-function correlation for the PT-inducing effects on rat mitochondria as deduced from the values of CRC, expressed as per cent of the control (CRC of untreated mitochondria).

Substructures DR282 (C-5) and DR067 (imide group) exhibited marginal effects (around 20% of CRC loss), both as independent units or when combined in analogue DR496 (both in *endo* or *exo* configurations). Analogue DR085 (C-7 plus imide group) was nearly as active as the NRB mixture while DR166 (C-7) displayed the highest PT-inducing effect. All NRB substructures tested were found to have a negligible effect on mitochondria from guinea pig and mouse (Table 2).



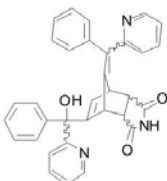
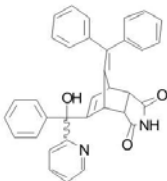
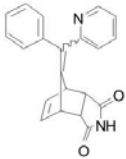
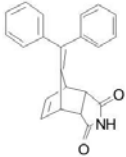
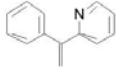
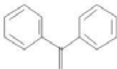
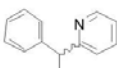
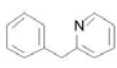
**Table 2. CRC of rat, mouse and guinea pig liver mitochondria in the presence of NRB and of the substructures: DR282, DR067, DR496(endo), DR496(exo), DR085, DR166.** The  $\text{Ca}^{2+}$  retention capacity (expressed as % of the control) was calculated according to the experimental procedure described in the legend to **Fig. 18**. Drug concentration was 50  $\mu\text{M}$ . Data are expressed as mean ( $\pm$  SD) of four independent determination

Structure	Compound	CRC (% of the control)		
		Rat	Mouse	Guinea Pig
	<b>DR282</b>	80 $\pm$ 10	90 $\pm$ 10	85 $\pm$ 5
	<b>DR067</b>	85 $\pm$ 10	100 $\pm$ 5	100 $\pm$ 5
	<b>DR496 endo</b>	80 $\pm$ 20	85 $\pm$ 10	90 $\pm$ 10
	<b>DR496 exo</b>	90 $\pm$ 10	85 $\pm$ 20	90 $\pm$ 10
	<b>DR166</b>	35 $\pm$ 5	90 $\pm$ 10	90 $\pm$ 5
	<b>DR085</b>	55 $\pm$ 5	90 $\pm$ 5	90 $\pm$ 10
	<b>NRB</b>	50 $\pm$ 10	100 $\pm$ 5	100 $\pm$ 10

The next set of experiments was aimed at investigating whether changes in the chemical structure of the most active compounds (NRB, DR085 and DR166) influenced their activity in rat mitochondria. To this purpose, we analyzed their analogues DR488, DR068 and DR598, in which the C-7 pyridyl ring was replaced by a phenyl ring, along with analogues of DR166, in which the terminal

methylene group was removed (DR303) or replaced by a methyl group (DR322). Table 3 reports the comparison between the CRC values of the modified analogues and the corresponding original molecules.

**Table 3. CRC of rat, mouse and guinea pig liver mitochondria in the presence of NRB and of the substructures: DR488, DR085, DR068, DR166, DR598, DR303, DR322.** The  $\text{Ca}^{2+}$  retention capacity (expressed as % of the control) was calculated according to the experimental procedure described in the legend to Fig. 18. Drug concentration was 50  $\mu\text{M}$ . Data are expressed as mean ( $\pm\text{SD}$ ) of four independent determinations.

Structure	Compound	CRC (% of the control)		
		Rat	Mouse	Guinea Pig
	<b>NRB</b>	50 $\pm$ 10	100 $\pm$ 5	100 $\pm$ 10
	<b>DR488</b>	80 $\pm$ 5	90 $\pm$ 10	90 $\pm$ 10
	<b>DR085</b>	55 $\pm$ 5	90 $\pm$ 5	90 $\pm$ 10
	<b>DR068</b>	85 $\pm$ 10	85 $\pm$ 10	85 $\pm$ 5
	<b>DR166</b>	35 $\pm$ 5	90 $\pm$ 10	90 $\pm$ 5
	<b>DR598</b>	85 $\pm$ 10	90 $\pm$ 10	95 $\pm$ 10
	<b>DR322</b>	70 $\pm$ 5	100 $\pm$ 5	75 $\pm$ 5
	<b>DR303</b>	85 $\pm$ 10	100 $\pm$ 5	90 $\pm$ 10

Chemical modifications to the original structures of the active compounds markedly reduced their PT-inducing activity. Thus, both the C-7 pyridyl N-atom and the terminal methylene group were important in conferring high PTP activation potential to the NRB molecule. Such modified NRB analogues were also ineffective in guinea pig and mouse mitochondria (Table 3).

#### 6.4. Mechanisms of species-selectivity towards the PT: species-specific differences in PTP structure or rather in drug transport?

##### 6.4.1. “Target” of NRB in the PTP. Experiments with cationic derivatives of NRB.

We next carried out a set of experiments with cationic derivatives of NRB, which should be able potentially to accumulate inside the mitochondria driven by the transmembrane potential (negative inside) of the inner membrane. Drug entry *via* mitochondrial membrane potential is possible only if the molecule is endowed with an appropriate degree of lipophilicity allowing it to cross the membrane. Using an alternative pathway for drug entry into mitochondria, as compared to the passive diffusion of the neutral molecule, we were aimed at better defining the properties of NRB target in the pore.

The following cationic analogues (OL14, JS023, DR380) based on the most active compounds (NRB and DR166) towards the PT were considered together with a cationic derivative (DR656) of the inactive analogue DR282 (Fig 22).

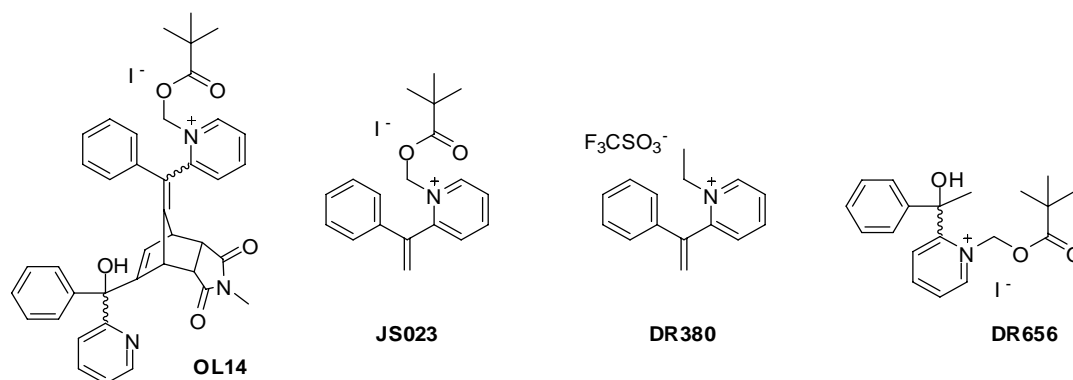


**Figure 22. Cationic derivatives of NRB, DR166 and DR282**

All the selected cationic NRB derivatives accumulated into the mitochondrial matrix, as tested by measuring the inner membrane potential through the fluorescence changes of Pyr G. As shown in Fig. 23, addition of succinate to de-energized rat liver mitochondria initiated a process of fluorescence quenching of Pyr G, which was due to accumulation of the probe inside mitochondria after energization (see Materials and Methods).

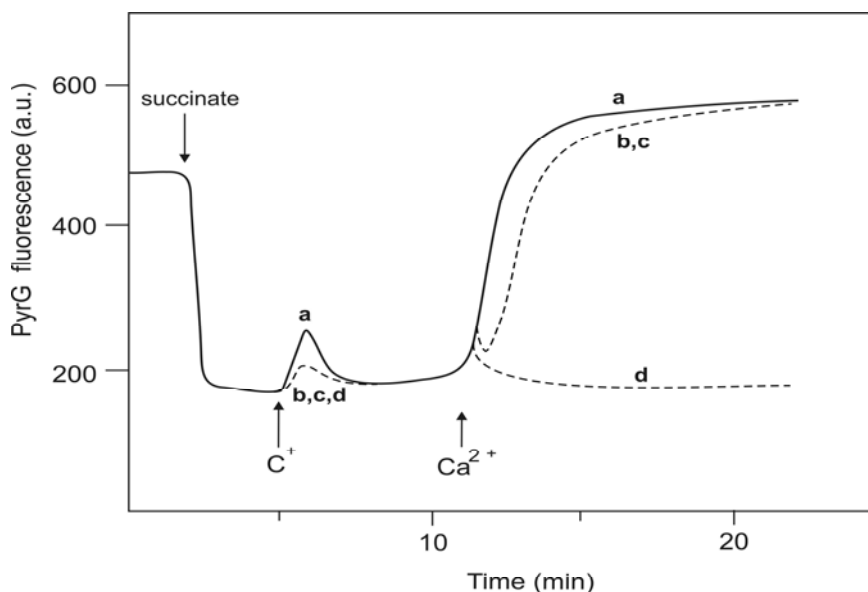


**Figure 23. Dependence of PyrG fluorescence on the mitochondrial membrane potential in the presence of cationic NRB derivatives (100  $\mu$ M).** Rat liver mitochondria (1 mg/ml), incubated with 3  $\mu$ M Pyr G, were suspended in the standard medium in the absence of an energizing substrate. Pyr G fluorescence (in arbitrary units) was followed by exciting at 520 nm (emission  $\lambda$ = 580 nm). Where indicated (arrows), succinate (5 mM), OL14 (trace a), JS023 (trace b), DR380 (trace c), DR656 (trace d) or  $\text{CaCl}_2$  (10  $\mu$ M) was added.

Addition of the cations ( $\text{C}^+$ , 100  $\mu$ M) OL14 (trace a), JS023 (trace b), DR380 (trace c) or DR656 (trace d) caused a cycle of probe release-reuptake, which indicates a transient membrane depolarization due to cation transport into the mitochondrial matrix. Addition of a small pulse of  $\text{Ca}^{2+}$  caused collapse of the membrane potential in mitochondria treated with OL14, JS023 and DR380. The collapse of membrane potential was not due to the addition of  $\text{Ca}^{2+}$  *per se* (e.g., trace d) but rather to PTP opening, as confirmed by the effect of CsA, which prevented the  $\text{Ca}^{2+}$ -dependent fluorescence increase (not shown). In contrast, only a transient depolarization due to  $\text{Ca}^{2+}$  transport in the matrix was observed

with DR656, whereas  $\text{Ca}^{2+}$  was ineffective. Similar results were obtained for mouse and guinea pig mitochondria (results not shown).

These findings suggest that all cationic derivatives were able to cross the rat mitochondrial membranes but only those bearing the “active core” of NRB molecule could stimulate the PT. In addition, “active” cationic derivatives were efficient towards the PT also in other animal species. These conclusions were supported by the following experiments of CRC determination.

Fig. 24 shows the CRC of rat mitochondria obtained in the presence of the selected cationic drugs at 50  $\mu\text{M}$  concentration, and compares the results to those obtained with the corresponding neutral analogues.

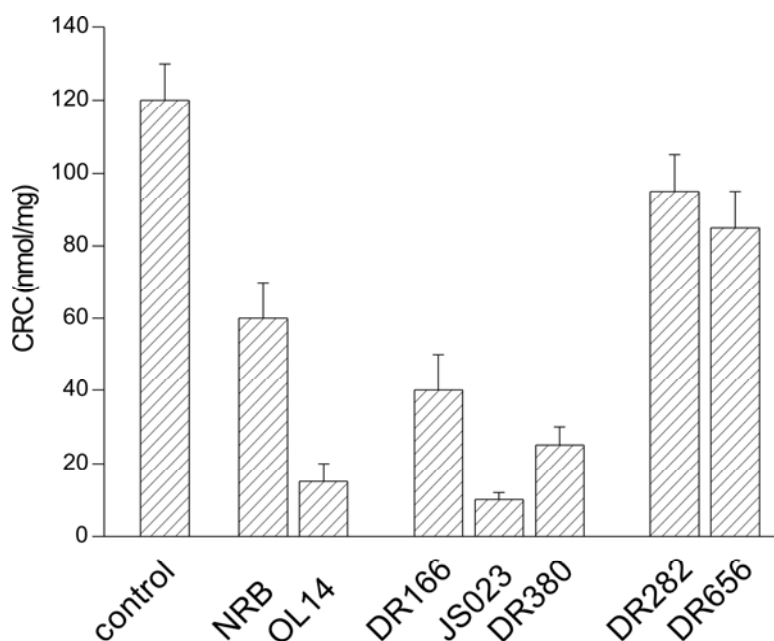


**Figure 24.** Comparison between the CRC of rat liver mitochondria loaded with the cationic compounds: OL14, JS023, DR380, and DR656 and their neutral analogues: NRB, DR166, and DR282. The concentration of all NRB derivatives was 50  $\mu\text{M}$ . The CRC was calculated according to the experimental procedure described in the legend to Fig. 18. Data are expressed as mean ( $\pm$  SD) of three independent determinations. Statistical analysis indicated that the data obtained in the presence of NRB, DR166, OL14, JS023, DR380 are significantly different from those of the control (unpaired t-test,  $P < 0.01$ ).

Clearly, the cationic derivatives of both the parent NRB molecule and of DR166 were much more effective in stimulating the PT than the neutral drugs. Indeed, the  $\text{Ca}^{2+}$  accumulated and retained before occurrence of the PT decreased from 40-60 nmol/mg to 10-30 nmol/mg. The cationic drugs bearing a *N*-pivaloyloxymethyl group (JS023 and OL14) displayed higher PT-inducing efficacy than displayed by the compound bearing a *N*-ethyl group (DR380), possibly as a consequence of a higher degree of lipophilicity. On the contrary, no significant changes in CRC were observed after insertion of a positive charge into DR282, thus confirming that this moiety does not affect the PT.

The dramatic increase in PT-inducing potency of the most active compounds after addition of a positive charge can be better evaluated by the dose-dependence data of Fig. 25, which compares, as an example, the CRC values of mitochondria supplemented with the cationic active “core” (JS023), with its neutral analogue (DR166) and with the parent molecule (NRB).

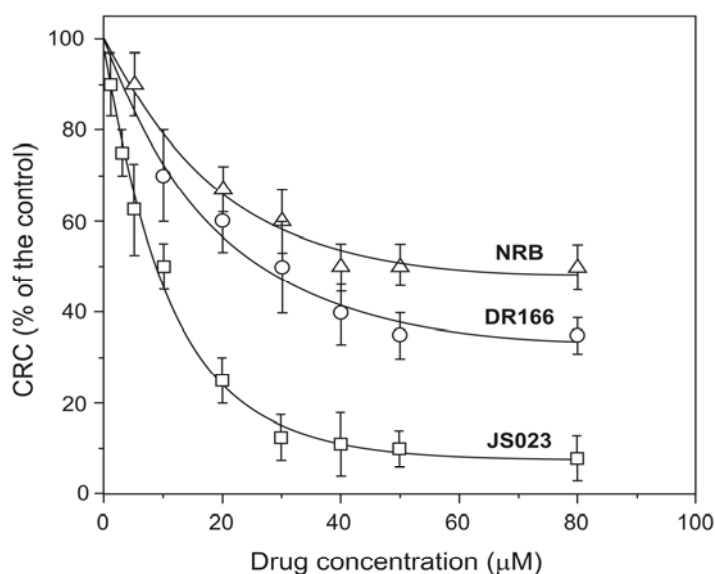


**Figure 25.** CRC of rat liver mitochondria loaded with increasing concentrations of JS023, DR166 and NRB. The CRC was calculated according to the experimental procedure described in the legend to Fig. 18. Data are expressed as mean ( $\pm$  SD) of three independent determinations.

The availability of active cationic derivatives which accumulate in the matrix provides a unique opportunity to test whether the lack of effects of NRB in mouse

and guinea pig mitochondria depends on species-specific differences in PTP structure or rather in drug transport. Accessibility of NRB substrate on the PTP also in species different from rat, provided that the drug is internalized by an appropriate pathway, was already evident from the results described in Fig 23.

In the next experiments we compared the effects of JS023 (Fig. 26A) and OL14 (Fig. 26B) on the CRC of rat and mouse mitochondria.

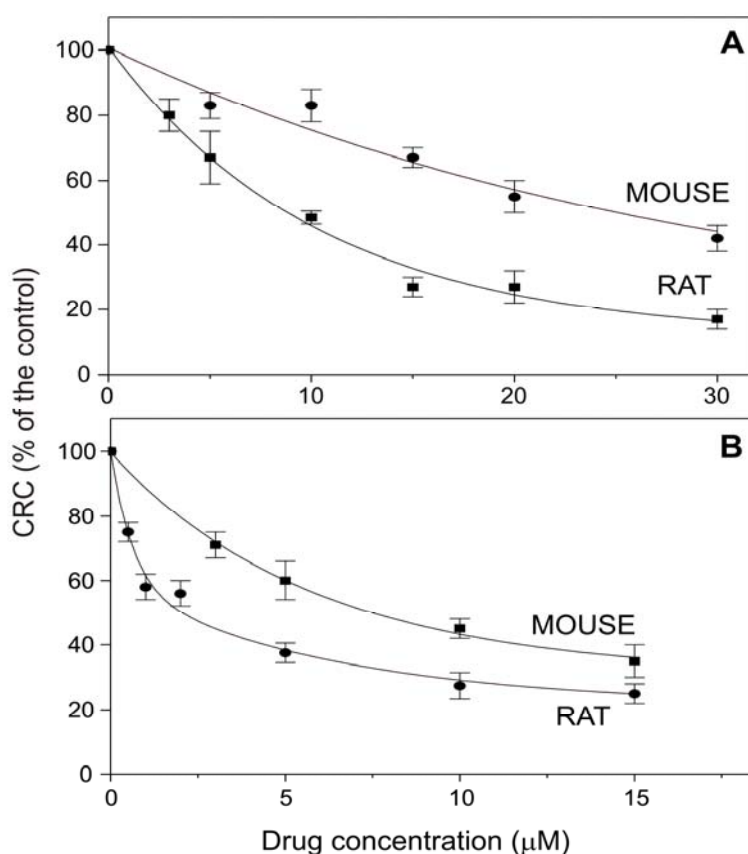


**Figure 26.** CRC of rat and mouse liver mitochondria in the presence of increasing concentrations of JS023 (A) and OL14 (B). The CRC was calculated according to the experimental procedure described in the legend to Fig. 1. CRC values are expressed as percentage of the corresponding controls (untreated mitochondria). Data are means ( $\pm$  SD) of three independent determinations. Results similar to those of mouse were obtained for guinea pig liver mitochondria.

It was confirmed that both cationic drugs were able to induce opening of the PTP also in mouse mitochondria, although higher concentrations were necessary to obtain effects similar to those observed in rat mitochondria. Similar results were

observed with guinea pig mitochondria (not shown). In conclusion, the species-specificity of PTP activation is lost when cationic NRB derivatives are used.

Clearly, the species-specificity of neutral NRB towards the mitochondrial PT cannot be ascribed to a difference in the nature of the drug target since the experiments with cationic drugs demonstrate that in all cases (rat and non-rat animal species) the (phenylvinyl)pyridine (DR166) moiety was necessary to induce the PT. On the other hand, the differences in PT-activation efficacy of cationic drugs suggest that some constrictions limitate the accessibility of the PTP-target in mitochondria of animal species different from rat.

#### *6.4.2. Transport modality of NRB into mitochondria. Fluorescence anisotropy measurements.*

In order to identify which membrane domains were perturbed by NRB and NRB We studied the dynamic properties of the mitochondrial membranes in the presence of NRB and NRB analogues by fluorescence anisotropy. In particular, we investigated whether the increase of PT-inducing efficacy correlated with a change in the distribution pattern of the drug in the membrane.

analogues, we measured the fluorescence anisotropy changes of DPH- and TMA-DPH-labelled mitochondria (in the presence of CsA to prevent opening of the PTP) (see Materials and Methods).

We compared the effects of the whole molecule with those of its active subunit, DR166, along with the cationic derivative JS023, at 50  $\mu$ M concentrations (Fig. 27). In rat mitochondria (panel A), NRB mostly affected the hydrophobic core of the lipid bilayer, as detected by the changes in DPH anisotropy. The decline of anisotropy intensity is indicative of an increase in lipid fluidity (Ricchelli *et al.*, 2005; Szöllösi, 1994). No relevant structural modifications of the polar heads/lipid backbone interface regions, as monitored by TMA-DPH anisotropy (Szöllösi *et al.*, 1994), were apparent. These data suggest a preferential accommodation of NRB in the interior of the lipid bilayer. In contrast, DR166 (panel B) mostly perturbed the lipid domains sensed by TMA-DPH, which suggests a preferential accumulation of this fragment in the lipid tail/polar heads border areas. Such lipid domains should mainly reside in the matrix-exposed



leaflet of the inner membrane bilayer since we found that TMA-DPH is transported in the inner membrane interior by charge effects (data not shown).

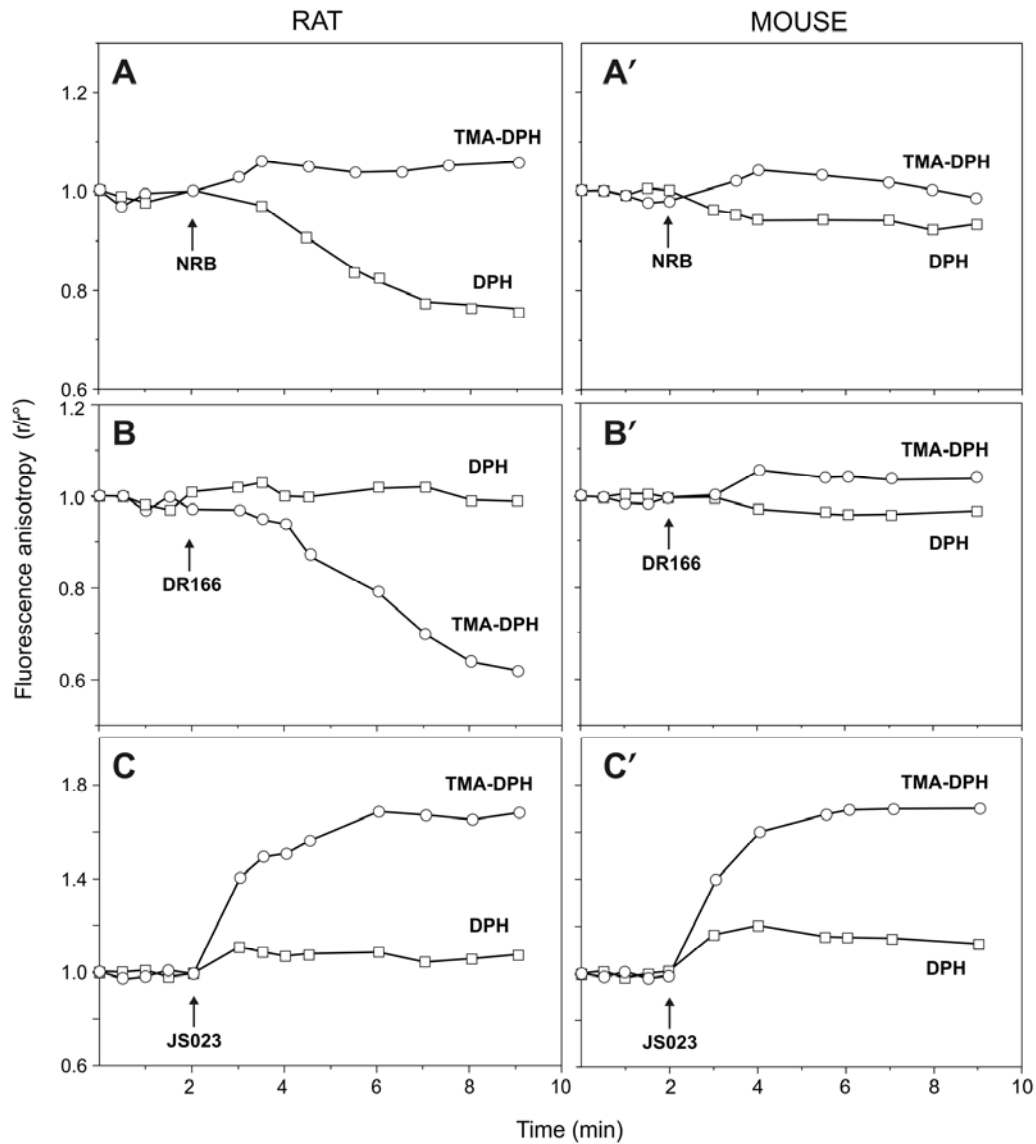


**Figure 27. Effects of NRB, DR166 and JS023 on the fluorescence anisotropy of DPH-, and TMA-DPH-labelled rat and mouse mitochondria.** DPH- and TMA-DPH-labelled mitochondria were prepared by treating mitochondrial suspensions (20 mg/ml) with 300  $\mu$ M probe. After 20 min (DPH) or 5 min (TMA-DPH) incubation under continuous stirring at  $T = 25^\circ\text{C}$ , the mitochondrial suspensions were diluted to 0.2 mg/ml for anisotropy measurements. The fluorescence anisotropies,  $r$ , were collected at 340 nm ( $\lambda_{em} = 460$  nm) (for DPH) and 360 nm ( $\lambda_{em} = 430$  nm) (for TMA-DPH). All anisotropy intensities were normalized to those ( $r^\circ$ ) observed before addition of 50  $\mu$ M NRB (A, A'), DR166 (B, B'), JS023 (C, C') (for rat mitochondria,  $r^\circ$ s of DPH and TMA-DPH were, respectively,  $0.14 \pm 0.01$  and  $0.09 \pm 0.02$ ; for mouse mitochondria the corresponding  $r^\circ$ s were:  $0.16 \pm 0.02$  and  $0.1 \pm 0.02$ ).

Accumulation of the cationic drug JS023 in the matrix-exposed regions caused a relevant increase of TMA-DPH anisotropy (panel C), which reflects a structural immobilization of these membrane domains, probably due to ionic interactions between JS023 and the negatively charged phospholipid heads. Similar effects were observed with other cationic NRB analogues, such as OL14 and DR380 (data not shown).

In mouse mitochondria (Fig. 27, panels A', B'), DPH and TMA-DPH reported only minor changes in the membrane dynamic properties upon interaction with the neutral compounds, NRB and DR166; on the other hand, the cationic analogue JS023 (panel C') exhibited effects similar to those observed in rat mitochondria.

The results described in Fig. 27 were obtained using elevated drug concentrations (50  $\mu\text{M}$ ). It is noteworthy that rat and mouse mitochondria displayed a marked difference in TMA-DPH anisotropy changes at increasing concentrations of JS023 below 50  $\mu\text{M}$  (Fig. 28).

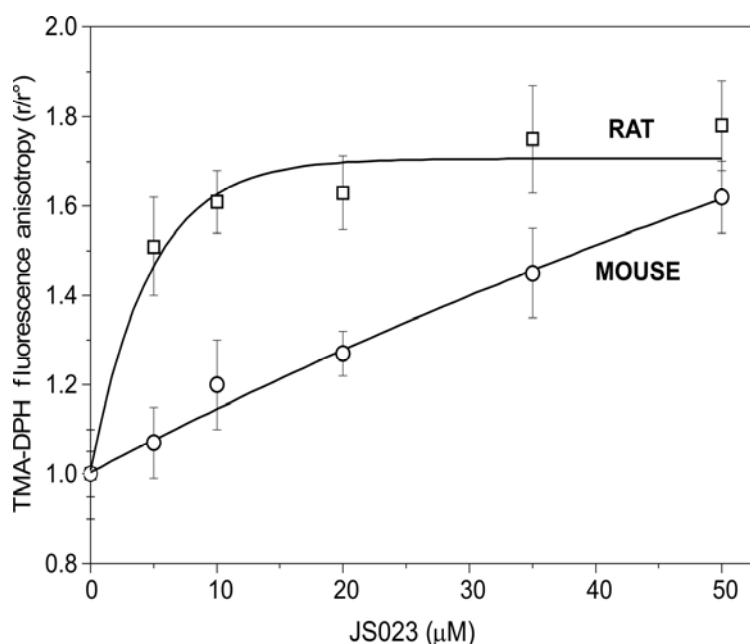


**Figure 28.** Effects of increasing concentrations of JS023 on the fluorescence anisotropy of TMA-DPH-labelled rat and mouse mitochondria. The experimental procedure was the same as described in the legend to Fig. 18. All anisotropy intensities were normalized to those ( $r^\circ$ ) observed before addition of JS023 (see legend to Fig. 18). Data are means ( $\pm$  SD) of three independent determinations.

With mouse mitochondria, higher concentrations of cationic drug were necessary to induce increases of the probe anisotropy comparable to those obtained in rat mitochondria. Strikingly, the dose-dependent anisotropy trend closely matched that obtained for PT induction (Fig. 28, compare with Fig. 26A).



## 7. DISCUSSION

The mechanisms underlying the rat-selective vasoconstriction effect and toxicity of NRB are still poorly understood. Detailed studies of the individual stereoisomers of NRB demonstrated that both drug-induced contractile activity and lethality in rats are strongly modulated by the molecular isomerism, only the *endo* configurations retaining the pathological effects elicited by the mixture (Brimble *et al.*, 2004). These results indicate that binding of NRB *in vivo* is stereospecific, thereby suggesting the existence of a drug receptor uniquely expressed in the myocytes of the rat peripheral vessels. Moreover, recent experiments on the rat caudal artery with selected fragments of the parent molecule demonstrated that groups at all three sites (C-7, C-5 and imide) must be retained for NRB-type vasoconstriction, the “*endo*-type” isomerism not being sufficient to cause toxic effects *per se* (Rennison *et al.*, 2007).

Intriguingly, NRB was recently shown to cause rat-selective opening of the PTP in isolated mitochondria (Ricchelli *et al.*, 2005), suggesting that *in vivo* mitochondrial dysfunction could be a potential physiological pathway leading to death in rats. To test this hypothesis, we evaluated the PT-inducing effects of rat-toxic (*endo*-isomers V, Y, W) and non toxic (*exo*-isomers R, X, T) compounds on isolated liver mitochondria. The results obtained from our experiments show that both lethal and non lethal NRB isomers display comparable stimulatory effects on the PT. Yet, all PTP-active isomers maintained a strict species-selectivity for the rat.

Although a direct correlation between NRB-induced mitochondrial dysfunction and lethal vasoconstriction is not obvious from these data, the possibility of PTP being a cause of toxicity in the rat cannot be totally dismissed. As a matter of fact, rat-selective PTP opening in isolated mitochondria suggests that NRB may specifically affect rat mitochondria *in vivo* as well. Indeed, studies on mitochondria isolated from liver of rats previously subjected to NRB stress showed that mitochondria were damaged to some extent and that energy-dependent reactions were impaired (Patil and Radhakrishnamurty, 1977). Very importantly, all compounds lethal to rats are also PTP-active in isolated mitochondria. Although we observed induction of the PT in isolated mitochondria

also by non-lethal NRB isoforms, our findings indicate that transport may be a key factor determining bioavailability to mitochondria *in situ*. Thus, the possibility exists that the exo-isomers do not reach mitochondria in the tissues that are critical for toxicity. An alternative hypothesis is that mitochondrial damage could play a role in NRB toxicity as a secondary, potentiating event.

In order to test whether the whole NRB molecule is necessary (as found for the vasoconstriction effect) or whether a specific active core is sufficient to account for the NRB effects on mitochondrial function, we assayed the PT-inducing efficacy of various NRB analogues, probing the parent molecule's three key structural features (substituents at C-5, C-7 and the imide unit). Our results indicate that neither the group at C-5 nor the imide group play a critical role in PT induction, whereas the (phenylvinyl)pyridine subunit at C-7 remains active, being sufficient for PTP activation. The possibility that this subunit is the key element conferring toxicity to NRB molecule also *in vivo* cannot be ruled out: actually, molecular integrity and *endo*-type stereoisomerism could be necessary for properly modulating the binding of NRB to its cell receptors, the whole molecular scaffold then functioning as a vector for the active feature responsible for the rat-unique effects. Clearly, further studies are necessary in order to better understand the mode of action and selectivity of NRB and the possible correlations between the different pathological effects.

If the hypothesis of a direct link between NRB-induced mitochondrial dysfunction and vasoconstriction is correct, a plausible mechanistic explanation should take into account the unique behaviour of the rat mitochondrial system towards the drug. The selectivity of PTP opening in isolated mitochondria, in fact, would suggest that the interaction mode of NRB in rat mitochondria is different from that taking place in mitochondria from other animal species *in vivo* as well. This difference could be due to a different pore structure/target or to a different modality of drug internalization. To better clarify this point, we used cationic derivatives of the drug which were shown to enter mitochondria driven by the inside-negative potential of the inner membrane. CRC experiments demonstrated that cationic NRB analogues can activate the PTP, provided that they bear the active core of the molecule, i.e. the (phenylvinyl)pyridine subunit. Under these conditions, mouse and guinea pig mitochondria are also affected by the drug. These findings clearly indicate that:

i) NRB as well as NRB substructures are endowed with an intrinsic ability to cross mitochondrial membranes in all animal species. This is not unexpected as the lipid composition of the mitochondrial membranes is similar between the different species,

ii) NRB target on the PTP is the same in all animal species since it specifically recognizes the (phenylvinyl)pyridine moiety. The need of higher drug concentrations for PT induction in mouse and guinea pig mitochondria, as compared to rat mitochondria, can be ascribed to a different distribution pattern of the drug in rat and non-rat species, as it can be deduced from the results of fluorescence anisotropy experiments.

The fluorescence anisotropy experiments, carried out with selected reporters of different membrane domains, indicate that the target of NRB action is localized on the matrix side of the mitochondria, which is in agreement with a preferential stimulation by NRB of the PTP-activating capacity of the internal  $\text{Ca}^{2+}$  site, as previously suggested (Ricchelli et al., 2005). Actually, the order of drug efficacy,  $\text{NRB} < \text{DR166} < \text{cationic NRB}$ , correlates very well with a gradual shift of drug distribution from the core of the lipid bilayer to matrix-exposed mitochondrial domains (Fig. 28). Furthermore, there is a strict correspondence between the extent of drug-induced perturbation of matrix lipid domains and the efficiency of PTP-activation (compare Fig. 28 and 26). Similar correlations between membrane-perturbing effects and PTP-triggering by cationic NRB derivatives can be observed in mouse and guinea pig mitochondria, which again suggests that the selectivity of NRB action on mitochondria does not concern the target of the drug on the pore. Rather, the higher doses of cationic drug necessary to induce perturbation of the matrix domains and PT activation, together with the inertness of neutral compounds, clearly indicate that NRB does not easily gain access to the mitochondrial matrix in any species other than the rat.

Taken together, these findings suggest that the amount of NRB taken up by mitochondria *via* passive diffusion may not be sufficient to perturb mitochondria and stimulate the PT. Thus, as previously suggested (Ricchelli *et al.*, 2005), the occurrence of PTP activation specifically in rats probably involves a transport system allowing a deeper penetration of the drug in the inner membrane.





## 8. BIBLIOGRAPHY

Basso E, Fante L, Fowlkes J, Petronilli V, Forte MA, Bernardi P (2005) Properties of the permeability transition pore in mitochondria devoid of Cyclophilin D. *J. Biol. Chem.* 280, 18558-18561.

Bova S, Travisi L, Debetto P, Cima L, Furnari M, Luciani S, Padrini R, Cargnelli G (1996) Vasorelaxant properties of norbormide, a selective vasoconstrictor agent of the microvasculature. *Br. J. Pharmacol.* 117, 1041-1046.

Bova S, Cargnelli G, D'Amato E, Forti S, Yang Q, Trevisi L, Debetto P, Cima L, Luciani S, Padrini R (1997) Calcium-antagonist effect of norbormide on isolated perfused heart and cardiac myocytes of guinea-pig: a comparison with verapamil. *Br. J. Pharmacol.* 120, 19-24.

Bova S, Trevisi L, Cima L, Luciani S, Golovina V, Cargnelli G (2001a) Signaling mechanisms for the selective vasoconstrictor effect of norbormide on the rat small arteries. *J. Pharmacol Exp. Ther.* 296, 458-463.

Bova S, Trevisi L, Cima L, Luciani S, Golovina V, Cargnelli G (2001b) Norbormide: a calcium entry blocker with selective vasoconstrictor activity in rat peripheral arteries. *Cardiovasc. Drug Rev.* 19, 226-233.

Bernardi P, Broekemeier KM, Pfeiffer DR (1994) Recent progress on regulation of the mitochondrial permeability transition pore; a cyclosporin-sensitive pore in the inner mitochondrial membrane. *J. Bioenerg. Biomembr.* 26, 509-517.

Bernardi P (1999) Mitochondrial transport of cations: channels, exchangers, and permeability transition. *Physiol. Rev.* 79, 1127-1155.

Bernardi P, Petronilli V, Di Lisa F and Forte M (2001) A mitochondrial perspective on cell death. *Trends Biochem. Sci.* 26(2), 112-117.

Bernardi P, Krauskopf A, Basso E, Petronilli V, Blalchy-Dyson E, Di Lisa F, Forte MA (2006) The mitochondrial permeability transition from *in vitro* artifact to disease target. *FEBS J.* 273, 2077-2099.

Bianchi K, Rimessi A, Prandini A, Szabadkai G, and Rizzuto R (2004) Calcium and mitochondria: mechanisms and functions of a trouble relationship. *Biochim. Biophys. Acta* 1742, 119-131.

Bossy-Wetzel E, Newmeyer DD, Green DR (1998) Mitochondrial cytochrome c release in apoptosis occurs upstream of DEVD-specific caspase activation and independently of mitochondrial transmembrane depolarization. *EMBO J.* 17, 37-49.

Brimble MA, Muir VJ, Hopkins B, Bova S (2004) Synthesis and evaluation of vasoconstrictor and vasorelaxant activity of norbormide isomers, *ARKIVOC*, vol. i, pp. 1,11.

Chelli B, Falleni A, Salvetti F, Gremigni V, Lucacchini A, Martini C (2001) Peripheral-type benzodiazepine receptor ligands: mitochondrial permeability transition induction in rat cardiac tissue. *Biochem. Pharmacol.* 60, 695-705.

Costantini P, Chernyak R, Petronilli V, Bernardi P (1996) Modulation of the mitochondrial permeability transition pore by pyridine nucleotides and dithiol oxidation at two separate sites. *J. Biol. Chem.* 271, 6746-6751.

Costantini P, Colonna R, Bernardi P (1998) Induction of the mitochondrial permeability transition by N-ethylmaleimide depends on secondary oxidation of critical thiol groups. Potentiation by copper-ortho-phenanthroline without dimerization of the adenine nucleotide translocase. *Biochim. Biophys. Acta* 20;1365(3):385-92.

Costantini P, Belzacq AS, Vieira HL, Larochette N, de Pablo MA, Zamzami N, Susin SA, Brenner C, Kroemer G (2000) Oxidation of a critical thiol residue of

the adenine nucleotide translocator enforces Bcl-2-independent permeability transition pore opening and apoptosis. *Oncogene*. 13;19(2):307-14.

Crompton M (1999) The mitochondrial permeability transition pore and its role in cell death. *Biochem. J.* 341, 233-249.

Desangher S and Martinou JC (2000) Mitochondria as the central control point of apoptosis. *Cell Biology*. 10, 367-377.

Duchen MR, Surin A, Jacobson J (2003) Imaging mitochondrial function in intact cells. *Methods Enzymol.* 361, 353-389.

Frey TG and Mannella CA (2000) The internal structure of mitochondria. *Trends Biochem Sci.* 25 (7), 319-324.

Frey TG, Renken CW, Perkins GA (2000) Insight into mitochondrial structure and function from electron tomography. *Biochim Biophys Acta.* 1555(1-3), 196-203.

Fusi F, Saponara S, Sgaragli G, Cargnelli G, Bova S (2002) Ca<sup>2+</sup> entry blocking and contractility promoting actions of norbormide in single rat caudal artery myocytes. *Br. J. Pharmacol.* 137, 321-328.

Fontaine E, Eriksson O, Ichas F, Bernardi P (1998) Regulation of the permeability transition pore in skeletal muscle mitochondria. Modulation by electron flow through the respiratory chain complex I. *J. Biol. Chem.* 273, 12662-12668.

Gincel D, Shoshan-Barmatz V (2004) Glutamate interacts with VDAC and modulates opening of the mitochondrial permeability transition pore. *J. Bioenerg. Biomembr.* 36, 179-186.

Gunter TE, Buntinas L, Sparagna G, Eliseev R and Gunter K (2000) Mitochondrial calcium transport: mechanisms and functions. *Cell Calcium*. 28(5-6), 285-96

He L, Lemasters JJ (2002) Regulated and unregulated mitochondrial permeability transition pore: a new paradigm of pore structure and function? *FEBS Lett.* 511, 1-7.

Helestrap AP and Davidson AM (1990) Inhibition of  $\text{Ca}^{2+}$ -induced large-amplitude swelling of liver and heart mitochondria by cyclosporin is probably caused by the inhibitor binding to mitochondrial-matrix peptidyl-prolyl cis-trans isomerase and preventing it interacting with the adenine nucleotide translocase. *Biochem. J.* 268, 153-160.

Halestrap AP, Woodfield KY, Connern CP (1997) Oxidative stress, thiol reagents, and membrane potential modulate the mitochondrial permeability transition by affecting nucleotide binding to the adenine nucleotide translocase. *J. Biol. Chem.* 272(6):3346-54.

Halestrap AP, McStay GP, Clarke SJ (2002) The permeability transition pore complex: another view. *Biochimie.* 84(2-3):153-66.

Hirsch T, Decaudin D, Susin SA, Marchetti P, Larochette N, Resche-Rigon M, Kroemer G (1998) PK11195, a ligand of the mitochondrial benzodiazepine receptor, facilitates the induction of apoptosis and reverses Bcl-2-mediated cytoprotection. *Exp. Cell. Res.* 241, 426-434.

Javadov S and Karmazyn M, (2007) Mitochondrial permeability transition pore opening as an endpoint to initiate cell death and as a putative target for cardioprotection. *Cell. Physiol. Biochem.* 20(1-4), 1-22.

Jennings RB, Ganote CE (1976) Mitochondrial structure and function in acute myocardial ischemic injury. *Circ. Res.* 38, 180-191.

Johans M, Milanesi E, Franck M, Johans C, Liobikas J, Panagiotaki M, Greci L, Principato G, Kinnunen PKJ, Bernardi P *et al.* (2005) Modification of permeability transition pore arginine(s) by phenylglyoxal derivatives in isolated mitochondria

and mammalian cells: structure-function relationship of arginine ligands. *J.Biol. Chem.* 280, 12130-12136.

Kanno T, Sato EE, Muranaka S, Fujita H, Fujiwara T, Utsumi T, Inoue M, Utsumi K (2004) Oxidative stress underlies the mechanism for  $\text{Ca}^{2+}$ -induced permeability transition of mitochondria. *Free Radic. Res.* 38(1):27-35.

Kokoszka JE, Waymire KG, Levy SE, Sligh JE, Cai J, Jones DP, MacGregor GR, Wallace DC (2004) The ADP/ATP translocator is not essential for the mitochondrial permeability transition pore. *Nature* 427, 461-465.

Kowaltowski AJ, Vercesi AE, Castilho RF (1997) Mitochondrial membrane protein thiol reactivity with N-ethylmaleimide or mersalyl is modified by  $\text{Ca}^{2+}$  : correlation with mitochondrial permeability transition. *Biochim. Biophys. Acta* 1318(3):395-402.

Krauskopf A, Eriksson O, Craigen WJ, Forte MA, Bernardi P (2006) Properties of the permeability transition in VDAC (-/-) mitochondria. *Biochim. Biophys. Acta* 1757, 590-595.

Kroemer G, Zamzami N, Susin SA (1997) Mitochondrial control of apoptosis. *Immunol. Today.* 18, 44-51.

Lacapere JJ, Delavoie F, Li H, Peranzi G, Maccario J, Papadopoulos V, Vidic B (2001) Structural and functional study of reconstituted peripheral benzodiazepine receptor. *Biochem. Biophys. Res. Commun.* 284, 536-541.

Li J, Wang J, Zeng Y (2007) Peripheral benzodiazepine receptor ligand, PK11195 induces mitochondria cytochrome c release and dissipation of mitochondria potential via induction of mitochondria permeability transition. *Eur J Pharmacol.* in press

Mannella CA, (2000) Our changing view of mitochondria. *J. Bioenerg. Biomembr.* 32, 1-4.

McStay GP, Clarke SJ, Halestrap AP (2002) Role of critical thiol groups on the matrix surface of the adenine nucleotide translocase in the mechanism of the mitochondrial permeability transition pore. *Biochem J.* 15;367(Pt 2):541-8.

Nakagawa T, Shimizu S, Watanabe T, Yamaguchi O, Otsu K, Yamagata H, Inohara H, Kubo T, Tsujimoto Y (2005) Cyclophilin D-dependent mitochondrial permeability transition regulates some necrotic but non apoptotic cell death. *Nature* 437, 652-658.

Nicolli A, Petronilli V, Bernardi P (1993) Modulation of the mitochondrial cyclosporin A-sensitive permeability transition pore by matrix pH. Evidence that the pore open-closed probability is regulated by reversible histidine protonation. *Biochemistry* 32, 4461-4465.

Nicholls DG (2005) Mitochondria and calcium signaling. *Cell calcium.* 38, 311-317.

Noji H, Yasuda R, Yoshida M, and Kinosita, (1997) Direct observation of the rotation of F1-ATPase. *Nature.* 386(6622), 299-302.

Orrenius S, (2007) Reactive oxygen species in mitochondria-mediated cell death. *Drug. Met. Rev.* 39(2-3), 443-455.

Papadopoulos V, Amri H, Boujrad N, Cascio C, Culty M, Garnier M, Hardwick M, Li H, Vidic B, Brown AS *et al.* (1997) Peripheral benzodiazepine receptor in cholesterol transport and steroidogenesis. *Steroids* 62, 21-28.

Pastorino JG, Simbula G, Gilfor E, Hoek JB, Farber JL (1994) Protoporphyrin IX, an endogenous ligand of the peripheral benzodiazepine receptor, potentiates

induction of the mitochondrial permeability transition and killing of cultured hepatocytes by rotenone. *J. Biol. Chem.* 269, 31041-31046.

Patil TN, Radhakrishnamurthy R (1977) Influence of norbormide on properties of rat liver mitochondria, *Indian J. Biochem. Biophys.* 14, 68-71.

Perkins GA and Frey TG (2000) Recent structural insight into mitochondria gained by microscopi. *Micron* 31, 97-111.

Petronilli V, Cola C, Massari S, Colonna R, Bernardi P (1993) Physiological effectors modify voltage sensing by the cyclosporin A-sensitive permeability transition pore of mitochondria. *J. Biol. Chem.* 268, 21939-21945.

Petronilli V, Costantini P, Scorrano L, Colonna R, Passamonti S, Bernardi P (1994) The voltage sensor of the mitochondrial permeability transition pore is tuned by the oxidation-reduction state of vicinal thiols. Increase of the gating potential by oxidants and its reversal by reducing agents. *J. Bio. Chem.* 17;269(24), 16638-42.

Poos GI, Mohrbacher RJ, Carson EL, Paragamian V, Puma BM, Rasmussen CR, Roszkowsky AP (1996) Structure-activity studies with the selective rat toxicant norbormide. *J. Med. Chem.* 9, 537-540.

Rasola A and Bernardi P. (2007) The mitochondrial permeability transition pore and its involvement in cell death and in disease pathogenesis. *Apoptosis.* 12, 815-833.

Rennison D, Hopkins B, Bova S, Zulian A, Cavalli M, Ricchelli F, Brimble MA (2007) Synthesis and activity studies of analogues of the rat selective toxicant norbormide. *Bioorg. Med. Chem.* 15(8), 2963-2974.

Ricchelli F, Dabbeni-Sala F, Petronilli V, Bernardi P, Hopkins B, Bova S (2005) Species-specific modulation of the mitochondrial permeability transition by norbormide. *Biochim Biophys Acta.* 1708(2):178-86

- Roszokwski AP, Poos GI, Mohrbacher RJ (1964) Selective rat toxicant. *Science*. 144, 412-413.
- Roszokwski AP (1965) The pharmacological properties of norbormide, a selective rat toxicant. *J. Pharmacol. Exp. Ther.* 149, 288-299.
- Saito M, Korsmeyer SJ, Schlesinger PH, (2000) Bax-dependent transport of cytochrome c reconstituted in pure liposomes. *Nat. Cell. Biol.* 2, 553-555.
- Schendel SL, Montal M, Reed JC (1998) Bcl-2 family proteins as ion-channels. *Cell Death Differ.* 5, 372-380.
- Schultheiss HP, Klingenberg M (1984) Immunochemical characterization of the adenine nucleotide translocator. Organ specificity and conformation specificity. *Eur. J. Biochem.* 143, 599-605.
- Scorrano L, Penzo D, Petronilli V, Pagano F, Bernardi P (2001) Arachidonic acid causes cell death through the mitochondrial permeability transition. Implication for tumor necrosis factor- $\alpha$  apoptotic signaling. *J. Biol. Chem.* 276, 12035-12040.
- Steel PJ, Brimble MA, Hopkins B, Rennison D (2004) Two stereoisomers of the rat toxicant norbormide. *Acta Crystallogr., C. Cryst. Struct. Commun.* 60 (Pt5). 374-376.
- Skulachev VP (2001) Mitochondrial filaments and clusters as intracellular power-transmitting cables. *Trends Biochem. Sci.* 26, 23-29.
- Szabo I, Zoratti M (1993) The mitochondrial permeability transition pore may comprise VDAC molecules. Binary structure and voltage dependence of the pore. *FEBS Lett.* 330, 201-205.



Szöllösi J (1994) Fluidity/Viscosity of Biological Membranes, in: S. Damjanovich, J. Szöllösi, L. Tròn, M. Edidin (Eds.), *Mobility and Proximity in Biological Membranes. CRC Press, Boca Raton.* 137-208.

Tomov T.Ch. (1986) Pyronin G as a fluorescent probe for the quantitative determination of the membrane potential of mitochondria. *J. Biochem. Biophys. Methods* 13, 29-38.

Vander Heiden MG, Chandel NS, Schumacker PT, Thompson CB (1999) Bcl-x prevents cell death following growth factor withdrawal by facilitating mitochondrial ATP/ADP exchange. *Mol. Cell* 3, 159-167.

Yelnosky J, Lawlor R (1971) Cardiovascular effect of norbormide. *Eur. J. Pharmacol.* 16, 117-119.

Zamzami N, Kroemer G (2001), The mitochondrion in apoptosis: how Pandora's box opens. *Mol. Cell Biol.* 2, 67-71.

Zoratti M and Szabo I (1995) The mitochondrial permeability transition. *Biochim. Biophys. Acta.* 1241(2), 139-176.